Theoretical and Applied Climatology (2022) 150:1385–1405
https://doi.org/10.1007/s00704-022-04233-y

RESEARCH

Performance of a regional climate model with interactive vegetation (REMO-iMOVE) over Central Asia

P. Rai[1] · K. Ziegler[1] · D. Abel[1] · F. Pollinger[1] · H. Paeth[1]

Received: 29 June 2022 / Accepted: 4 October 2022 / Published online: 14 October 2022

Abstract

The current study evaluates the regional climate model REMO (v2015) and its new version REMO-iMOVE, including interactive vegetation and plant functional types (PFTs), over two Central Asian domains for the period of 2000–2015 at two different horizontal resolutions (0.44° and 0.11°). Various statistical metrices along with mean bias patterns for precipitation, temperature, and leaf area index have been used for the model evaluation. A better representation of the spatial pattern of precipitation is found at 0.11° resolution over most of Central Asia. Regarding the mean temperature, both model versions show a high level of agreement with the validation data, especially at the higher resolution. This also reduces the biases in maximum and minimum temperature. Generally, REMO-iMOVE shows an improvement regarding the temperature bias but produces a larger precipitation bias compared to the REMO conventional version with interannually static vegetation. Since the coupled version is capable to simulate the mean climate of Central Asia like its parent version, both can be used for impact studies and future projections. However, regarding the new vegetation scheme and its spatiotemporal representation exemplified by the leaf area index, REMO-iMOVE shows a clear advantage over REMO. This better simulation is caused by the implementation of more realistic and interactive vegetation and related atmospheric processes which consequently add value to the regional climate model.

1 Introduction

The countries Kazakhstan, Kyrgyzstan, Tajikistan, Turkmenistan, and Uzbekistan as well as the Xinjiang province of China altogether comprise Central Asia, covering an area close to 5 million km^2. The climate of this region is amongst the most sensitive climate zones around the world which also contains one of the largest drylands (Seddon et al. 2016). Observational data reveal general warming in mean annual temperature which ranges between 0.18 and 0.42 °C per decade in Central Asia (Unger-Shayesteh et al. 2013). The following decrease in the glaciated area in the Tian Shan (Aizen et al. 2007; Duishonakunov et al. 2014; Kenzhebaev et al. 2017), and Pamir-Alay (Hagg et al. 2007; Chevallier et al. 2014) mountain system in the south and the drying of the Aral Sea in the north contribute to increased water stress caused by the reduction of these important water storages. Additionally, there is a very high precipitation variability along with non-consistent trends on small scales due to the heterogeneity of the land surface (Lioubimtseva et al. 2005). The decrease of water resources along with the partially intense agricultural production, which has decreased quantitatively over the last few decades, are exposed to a growing risk with respect to climate change (Perelet 2007). There is increased water stress, especially in Kyrgyzstan and Uzbekistan with its high population (Pritchard 2017) which also influences the socio-economic development and enhances the potential of conflicts about food security (Fischer et al. 2005; Reyer et al. 2017). Hence, it is of utmost importance to improve the spatio-temporal climate variability in climate models for articulating regional adaptation and mitigation strategies considering the expected threats from climate change (Huang et al. 2014).

In order to dynamically downscale the coarser scale global climate simulations of General Circulation Models (GCMs) to a finer and regional scale, Regional Climate Models (RCMs) have proven to be a useful tool in the last few decades since they are able to represent complex land surface variables like orography and vegetation in more detail (e.g. Prein et al. 2015; Rummukainen et al. 2015; Giorgi and Gao 2018). By using the lateral boundary

✉ P. Rai
praveen-kumar.rai@uni-wuerzburg.de

[1] Institute of Geography and Geology, University of Würzburg, Würzburg, Germany

conditions of either GCMs or reanalysis, which act as so-called perfect boundary conditions, the lateral forcing is done (Wang et al. 2004). These models have been used in impact assessment studies and led to a better understanding of the climatic processes on regional scales in various parts of the world (e.g. Mannig et al. 2013; Kumar et al. 2020). However, increasing the resolution and complexity of the RCMs leads to the necessity to put extensive efforts into their continuous development and improvement (Giorgi 2019). Despite this enormous effort and known limitations like the dependence of the model's quality on the boundary conditions and the physical parameterizations (Paeth et al. 2005, 2009; Rummukainen 2010), using RCMs and dynamically downscale spatially coarse information has a clear advantage over statistical downscaling. The statistical downscaling is based upon the empirical relationship between several predictors and a variable of interest, which requires significantly fewer computing resources. However, the results are not achieved on a physical basis, which leads to problems when it comes to the investigation of time periods without observational data and in the generation of more consistent and comprehensive datasets.

Although Central Asia is a hotspot of climate change, only a few modeling studies have tried to investigate the climatological features in that region, including temperature and precipitation (Small et al. 1999; Lee and Suh 2000; Fu et al. 2005). One reason for that is the sparse and uneven distribution of meteorological stations in Central Asia which is challenging for the model validation since gridded validation data is negatively affected by a low station density (e.g., Hofstra et al. 2010; Prein and Gobiet 2017; Gibson et al. 2019). Regarding the existing modeling studies, some indicate the rising trend of temperature along with an increased precipitation variability in the region (Mannig et al. 2013; Li et al. 2015). Recently, Top et al. (2021) evaluated the performance of the regional climate models REMO and ALARO-0 over the Coordinated Regional Climate Downscaling Experiment domain of Central Asia (CORDEX-CAS) at a resolution of 0.22° and for the period of 1980–2017. They found a better performance of REMO in simulating the temperature while the ALARO-0 was better at simulating the precipitation over Central Asia. Russo et al. (2019) ran and evaluated the COSMO-CLM 5.0 at the resolution of 0.22° over CORDEX-CAS and find their model to be more sensitive to the parametrizations that deals with soil and surface properties. Ozturk et al. (2012, 2016) used the RegCM model at 0.44° for the climate projection with different emission scenarios for the period of 1971–2100. However, there is still a need for high-resolution datasets from the climate models over the CORDEX-CAS region in order to conduct environmental assessment applications along with impact modelling (Kotova et al. 2018). Additionally, Gessner et al. (2013) highlighted the sensitivity of the vegetation's development on precipitation over about 80% of Central Asian land surfaces, particularly in areas with annual precipitation ranging between 100 and 400 mm. Consequently, the present study is an attempt to generally broaden our knowledge of model performances over Central Asia for the RCM REMO. A specific focus lies on the effect that the coupling of an interactive vegetation model has on the performance of REMO.

As already mentioned, and also suggested by various studies in the past, the quality of the simulated climate can be highly influenced by the representation of land surface processes within climate models. Since the RCM REMO (v2015, Jacob et al. 2012) considers vegetation whose characteristics vary on the intra-annual scale but not inter-annually, there is a need for improvement. For this purpose, we consider the coupling of REMO with an interactive mosaic-based vegetation (iMOVE) scheme proposed by Wilhelm et al. (2014), called REMO-iMOVE. With the new land surface scheme, the phenology reacts directly to simulated weather and climate conditions instead of being static. This new scheme has been used for different land use and land cover studies as well as RCM comparisons over Europe (Breil et al. 2020; Davin et al. 2020; Sofiadis et al. 2021).

For the current study, iMOVE is implemented and adapted for the first time out of Europe. Additionally, the target resolution is higher than any comparable RCM study done for Central Asia which becomes possible since we perform the model simulations ourselves. Thus, the aim of this paper is to validate the performance of REMO and iMOVE and to show the effect of the new interactive vegetation, has on temperature and precipitation. We are particularly interested in the representation of the leaf area index and the mean temperature and precipitation variability of the two model versions. Additionally, the investigation is undergone for two different horizontal resolutions to estimate the effect of the higher spatial resolution in the heterogeneous land surface of Central Asia. This work is fundamental to estimate the model biases and shortcomings when it comes to the investigation of future projections.

The paper is organized as follows: In Section 2, we will present the model description and experimental design as well as the datasets used to validate the model and the related validation metrices. Section 3 contains a detailed description of the results we obtained which are discussed in Section 4. The conclusion and summary are done in Section 5.

2 Methodology

2.1 Model description

In this study, we use the three-dimensional and hydrostatic RCM REMO2015 (Jacob and Podzun 1997; Jacob 2001; Jacob et al. 2012). Its dynamical core is based on

the GCM ECHAM4 (Roeckner et al. 1996), although numerous improvements have been made since (e.g., Hagemann 2002; Semmler et al. 2004; Pfeifer 2006; Kotlarski 2007; Teichmann 2010; Wilhelm et al. 2014). The prognostic variables on 27 atmospheric levels are surface pressure, wind speed, specific humidity, air temperature, cloud liquid water, and ice. REMO has been successfully adapted to Central Asia in its former version REMO2009 (Mannig et al. 2013; Paeth et al. 2015) and in the frame of CORDEX and CORDEX-CORE (Giorgi et al. 2021) where it has shown that it can capture the features of the Central Asian climate well.

Wilhelm et al. (2014) have coupled REMO (v2009) with the dynamic land surface scheme JSBACH (Jena Scheme for Biosphere–Atmosphere Coupling in Hamburg) (Reick et al. 2013). JSBACH was developed in order to improve the efficiency of GCMs towards Earth System Models (ESMs) (for further details about JSBACH, we refer to Reick et al. (2013) and the explanation of its adaptation in Wilhelm et al. (2014)). Because of many advantages of JSBACH, such as its similarity in coding with REMO and its ability to exchange surface fluxes on model time step basis, it was adapted to REMO. Apart from the carbon pool parametrization, the iMOVE version includes all biophysical parameterizations for vegetation modelling from JSBACH, including precompiled Plant Functional Types (PFTs).

The introduction of PFTs by the coupled iMOVE-version is one of the most relevant advancements towards the coupling process. Based upon the comparable functional peculiarity and biophysical characterization, different plant species are aggregated to constitute the PFTs. Due to the aggregation, there is the possibility of choosing and handling a small but a representative number of functional types which may coexist inside a model grid box. Up to 16 PFTs which represent different biophysical biome characteristics (net primary productivity, stomatal conductance, surface albedo, rooting depth, leaf area index) can be represented within a single grid cell (Wilhelm et al. 2014).

The GLOBCOVER 2000 (GLC2000) dataset with a horizontal resolution of 1 km × 1 km is used to distribute the PFT classes horizontally (Bartholome and Belward 2005). GLC2000 also contains mixed vegetation classes such as shrubs and a mixture of trees, which need to be separated, along with classes such as needle leaf trees, which can be mapped into PFTs directly. Additionally, the climate zones following Holdridge (1967) are considered for the global distribution of PFTs. In the present study, the coupled version of REMOv2015 and iMOVE is used for the first time in Central Asia / out of Europe. The authors refer to Wilhelm et al. (2014) for further details on JSBACH and iMOVE.

2.2 Experimental design

A total of four simulations, two each with REMO and iMOVE on two different spatial resolutions, are performed over Central Asia for a period of 16 years starting from January 2000 till December 2015. The time step for the coarser runs (0.44°) is 240 s while it is 60 s for the 0.11° runs. The resolutions are run on two different domains (cp. Figure 1) from which the area of the inner domain is clipped from the coarse resolution runs when it comes to the comparison of different spatial resolutions. This inner domain is called CAS-44. The inner domain with 0.11° resolution was created to better resolve the land surface characteristics and small-scale meteorological processes. The ERA-Interim dataset with a horizontal resolution of 80 km (0.75°) (Dee et al. 2011) has been used to force the models at their lateral boundaries with an update frequency of 6h. There is a necessity for a spin-up period in order to allow the model and its inert land surface variables accommodate to the model internal physics and forcing (Giot et al. 2016). For this purpose, the model ran as a cold-start with the initial values from the forcing data for the period of 2000–2015 to spin up the lower-frequency variables like soil moisture and soil temperature which are

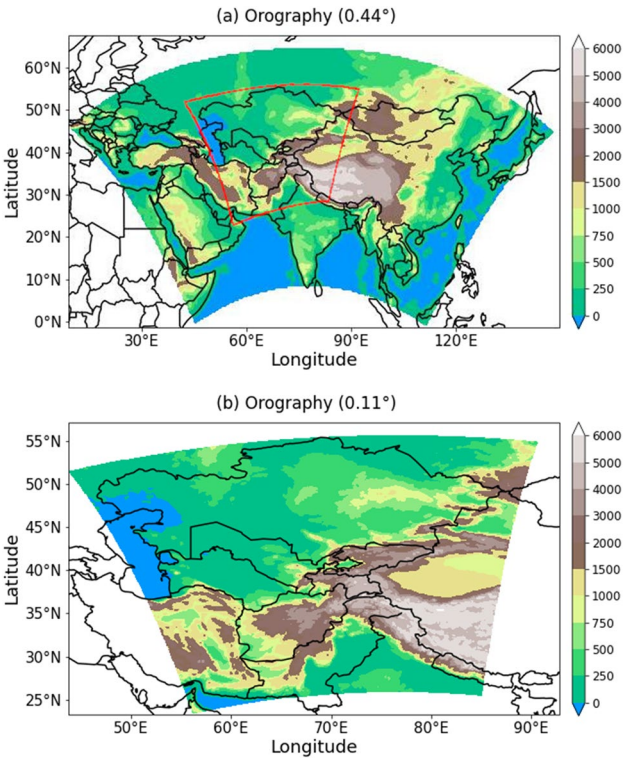

Fig. 1 Model domain with orography (m). **a** 0.44° (3.2°N to 61.1°N and 16°E to 141.6°E), and **b** 0.11° (24.3°N to 54.7°N and 45.6°E to 88.9°E) resolution. The red box in **a** marks the smaller domain within the larger domain

not in an equilibrium state. According to Sieck (2013), the state of the spin-up variables is taken from the end of the cold-start simulation and replaces one of the first forcing steps at the beginning of the simulations.

2.3 Observational and reanalysis datasets

For the purpose of model validation, various observational and reanalysis datasets have been used in the present study. To validate the simulated precipitation, the rain gauge measured and gridded Global Precipitation Climatology Centre (GPCC, v2018) data (Schneider et al. 2018) from the German Weather Service has been used in monthly form. We have used a horizontal resolution of 0.25° of GPCC to compare the model simulated precipitation after remapping them to the model grids of 0.44° and 0.11°. In general, GPCC data underestimate the precipitation during springtime and in mountainous regions (Hu et al. 2018). However, Hu et al. (2018) also reported a higher similarity of GPCC with observed station data in comparison to Climate Research Unit (CRU) and Matsuura-Wilmott (MW) precipitation data over Central Asia. Following Top et al. (2021), who have already used different observational datasets for comparison, we went for the bias calculation based on only one gridded dataset, which showed good results in their study, i.e., GPCC for precipitation and CRU for temperature.

To validate the temperature at 0.11°, the ERA5-Land reanalysis dataset from the European Centre for Medium-Range Weather Forecasts (ECMWF) is taken, having a native resolution of $0.1° \times 0.1°$ has been used (Muñoz Sabater 2019). This reanalysis product is available from 1950 to the present and is a specialized version of ERA5 with a series of improvements making it more accurate for all types of land applications. Generally, reanalysis datasets are more continuous in space and time than station data, but they do contain biases as well such as overestimation of precipitation globally and especially in mountainous regions (Sun et al. 2018).

To take the plant dynamics of iMOVE into account, the Leaf Area Index (LAI) of the model is considered. The LAI is a critical variable of an ecosystem to scale various plant-related processes such as transpiration, respiration, and photosynthesis. It is defined as the total one-sided leaf area per unit of ground area and therefore acts as a strong indicator of volumetric biomass within an ecosystem (Asner et al. 1998; Jarlan et al. 2008). For the validation, the Advanced Very High-Resolution Radiometer (AVHRR) sensors' LAI daily data at $0.05° \times 0.05°$ grids (1983–2017) is used from the National Climatic Data Centre (Vermote and NOAA CDR Program 2019). One shortcoming of AVHRR is that there is no data whenever cloud cover is present.

2.4 Statistical methods

For the comparison of variables simulated by the model, which have a different grid size with the observation and re-analysis datasets, interpolation is required to get the variables on a common grid (Kotlarski et al. 2014). In this study, we have used bilinear interpolation from the grids of observational and reanalysis datasets, respectively, to the original model grids. REMO's output variables are available at an hourly interval. Convective and stratiform rain variables are accumulated to get the monthly, seasonal, and annual sums of precipitation. LAI, mean, maximum, and minimum temperatures are taken from the hourly scale to seize their monthly, seasonal, and annual means. The spatial patterns of seasonal and annual biases from the monthly values are computed for the period from 2000 to 2015. The mean annual cycle of precipitation is calculated to assess the intra-annual variability in REMO and iMOVE.

The comparison of model performances with validation data is facilitated through the computation of different statistical metrics. E.g., the Index of Agreement (IOA) by Willmott (1982) is calculated as:

$$IOA = 1 - \frac{\sum (F_i - O_i)^2}{\sum \left(|F_i - \overline{O}| + |O_i - \overline{O}|\right)^2}$$

where F_i and O_i represent the forecast and validation data for the i^{th} year, respectively, while $\overline{O}$ is the climatological mean of the validation. The range of IOA is between 0 and 1, where a value of 1 represents the perfect index score with the best performance. In order to summarize the mean difference between observed and model simulation, the root mean squared error (RMSE) is quite effective. For the validation of precipitation, we use the normalized RMSE (NRMSE) that relates the RMSE to the mean value of the observed precipitation. The closer the NRMSE value is to 0 the better the score.

3 Results

The monthly, seasonally December-January–February (DJF; Winter), March–April-May (MAM; Spring), June-July–August (JJA; Summer), September–October-November (SON; Autumn), and annually averaged values for LAI, precipitation, and temperature are compared with the respective reference datasets.

3.1 LAI

The annual bias of the LAI in REMO and iMOVE with respect to AVHRR and the differences between the simulations are shown in Fig. 2 for the 0.44° (a, b, and c) and 0.11° (d, e, and f) domains, respectively. Taking the coarse resolution into account, the bias between the two REMO versions and AVHRR—where AVHRR is available—is either similar or lower which is also true for the seasons (Fig. s3) and in most subregions by using iMOVE. The only exceptions to this are related to smaller areas in south-eastern Russia and some local, tropical areas. The difference in the REMO versions further shows a strong decline in LAI in Southeast Asia and India (all seasons) and in most parts of China (JJA), where no AVHRR data exist. The reduction of the LAI is also present in the 0.11° resolution where only some northern areas of Kazakhstan and Afghanistan reveal higher biases in iMOVE than in REMO compared to AVHRR across most seasons (Fig. s4). Lowering the LAI values generally leads to a bias reduction. However, it has to be mentioned that the bias is not only reduced but becomes negative mainly during MAM and JJA in some Central Asian countries.

The investigation of the annual cycles of LAI for REMO and iMOVE and their comparison with the AVHRR data along with its temporal variation at 0.44° and 0.11° resolution is shown in Fig. 3a, b, and c, respectively. At both resolutions, iMOVE matches better with AVHRR in terms of magnitude than REMO does. For the coarser resolution and larger domain, it can be stated that REMO captures the annual cycle better than iMOVE which is due to the lower decline of LAI in SON. Nevertheless, iMOVE shows a good agreement of the annual cycle in the CAS-11 domain where most tropical areas are excluded. We conclude that the reduction of the LAI-bias within iMOVE is an advantage over REMO which is to be expected since a more advanced vegetation parameterization is used in this model version. Similar findings regarding the seasonal variations of LAI were also reported by Wilhelm et al. (2014). They described it as a result of the interactive coupling of LAI directly to its atmospheric and hydrological drivers in iMOVE, whereas REMO is based on a static annual cycle for LAI.

This behaviour is clearly shown in Fig. 3c. Here, a constant time series of annual LAI means shows the static vegetation of REMO and a consistent overestimation. The introduction of iMOVE leads to the representation of interannually varying LAIs. Thus, this is a clear improvement regarding the realisation of LAI variable where the more complex interactive vegetation scheme adds value compared to the former version. The comparison with AVHRR shows that the more realistic behaviour in addition to the general lowering of the values is also an absolute improvement of the model's representation of vegetation characteristics. It can be also stated that the finer resolution shows a generally lower bias than the coarse one.

3.2 Precipitation

Precipitation over the oceanic areas of the 0.44° domain has been masked in order to focus on the land areas. The monthly mean relative bias for seasonal and annual total precipitation from the simulations at 0.44° is based on remapped GPCC data and is shown in Fig. 4. The larger 0.44° domain accounts for the precipitation from different monsoon regions, especially the East Asian and South Asian Monsoon (SAM) systems. As far as Central Asia is concerned, the precipitation's spatial pattern and magnitude are mostly determined by its location between a northern temperate and southern subtropical climate along with its continentality. The large-scale circulation, especially jet streams

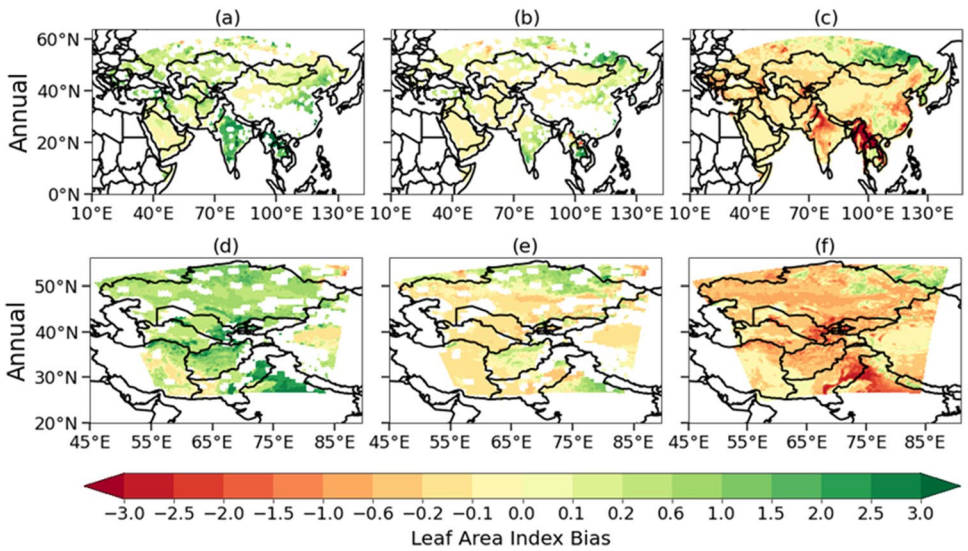

Fig. 2 **a**–**f** Mean monthly leaf area index bias (0.44°) for the period 2000–2015. Bias is calculated with respect to AVHRR. The last column shows the difference between iMOVE and standard REMO simulation runs

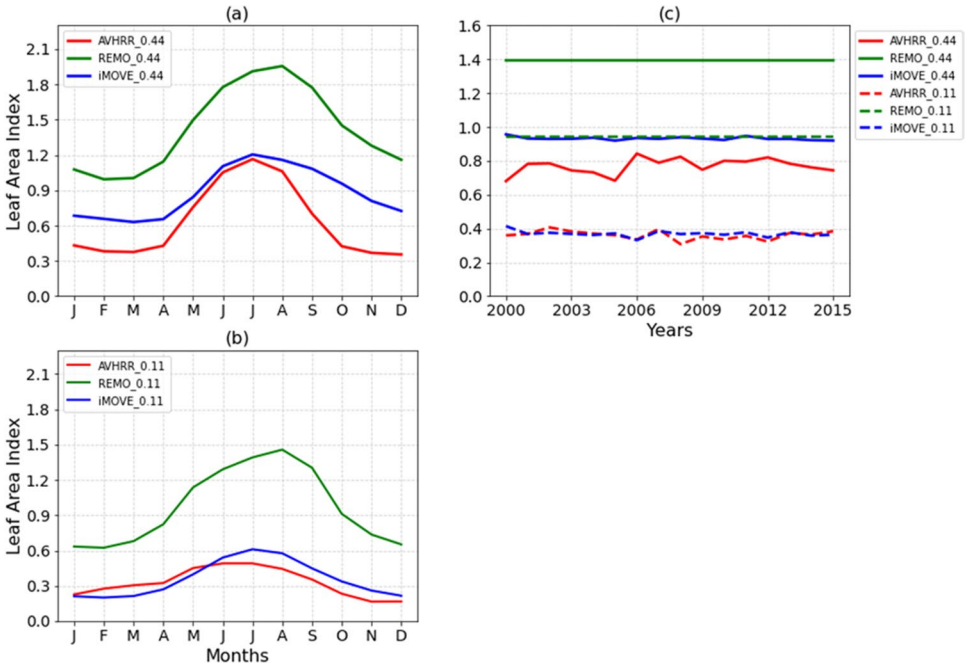

Fig. 3 **a–c** Mean annual cycle of leaf area index averaged over the model domains (0.44° and 0.11°) for the period 2000–2015

whose location is changing over the year, is an important factor in controlling the seasonal precipitation over Central Asia. Located over the northern part of the domain during summer, it moves to the south of Central Asia during winter. This leads to an extension of the Siberian High into the northern part of the model domain. Additionally, the overlying jet streams are responsible for the less stable weather conditions in the southern part.

All important climatological features of the precipitation pattern such as mountain ranges with higher amount of precipitation, the drier Central Asian plains and Tarim Basin, and the belt of very high precipitation in the Tibetan Plateau region occur in both models and observations (not shown). The bias pattern shows a slight wet bias in precipitation during the winter season over the Central Asian plains in both REMO and iMOVE, while precipitation is highly overestimated over higher-elevation regions, especially over the Tibetan Plateau and in southern and north-eastern parts of the domain (Fig. 4a and b). The drier regions like the Gobi Desert and Taklamakan are partially the reason for the large wet bias in winter as stated by Top et al. (2021). A similar pattern of wet bias during the winter season in REMO is also reported by Mannig et al. (2013) and Top et al. (2021). Russo et al. (2019) found a similar behaviour using the COSMO-CLM. The wet bias persists in the northern part of Central Asia during spring and, with slightly higher magnitude, in summer (Fig. 4d, e, g, and h).

Interactive vegetation in iMOVE produces a higher wet bias during summer as compared to REMO over Central Asia. Both models, especially iMOVE, are simulating a very large dry bias over the central and northern Indian regions. It shows the deficiency of both models in capturing the SAM system properly. The early monsoon onset in the models can be a possible reason for the dry bias during summer in India. Over the Mongolian region, a large wet bias can also be seen during summer which further intensifies in autumn. The lowest bias can be seen during autumn in both models (Fig. 4j and k). Since the wet biases are quite erroneous over the southern and north-eastern part of the domain, the absolute bias for precipitation is presented in the supplementary figure (Fig. s5a and b), where the overestimation during winter is quite small compared to the large relative bias shown in Fig. 4. In summary, iMOVE tends to enhance the precipitation bias compared with the REMO standard version across southern Asia.

A wet bias similar to the 0.44° simulation is present during the winter season over the Central Asian plains at 0.11° but with a lower magnitude as shown in Table 1. Furthermore, it is restricted mostly to the central, northern, and north-western parts of the domain (Fig. 5a and b) while most of the Central Asian plains are occupied by a dry bias during spring (Fig. 5d and e). A dry bias is present over the south-western part of the domain during all seasons. A decreased wet bias during summer as compared to the 0.44° resolution can be observed over the northern part of the domain, which is again slightly higher in iMOVE than REMO, while improvements in the orographic precipitation are also visible (Fig. 5g and h). Except for the southern slopes of the Himalayan region, where a large wet bias persists, northern India and most parts of Pakistan show a dry bias during the summer monsoon season. Again, the least amount of precipitation bias is present during autumn (Fig. 5j and k), whereas a

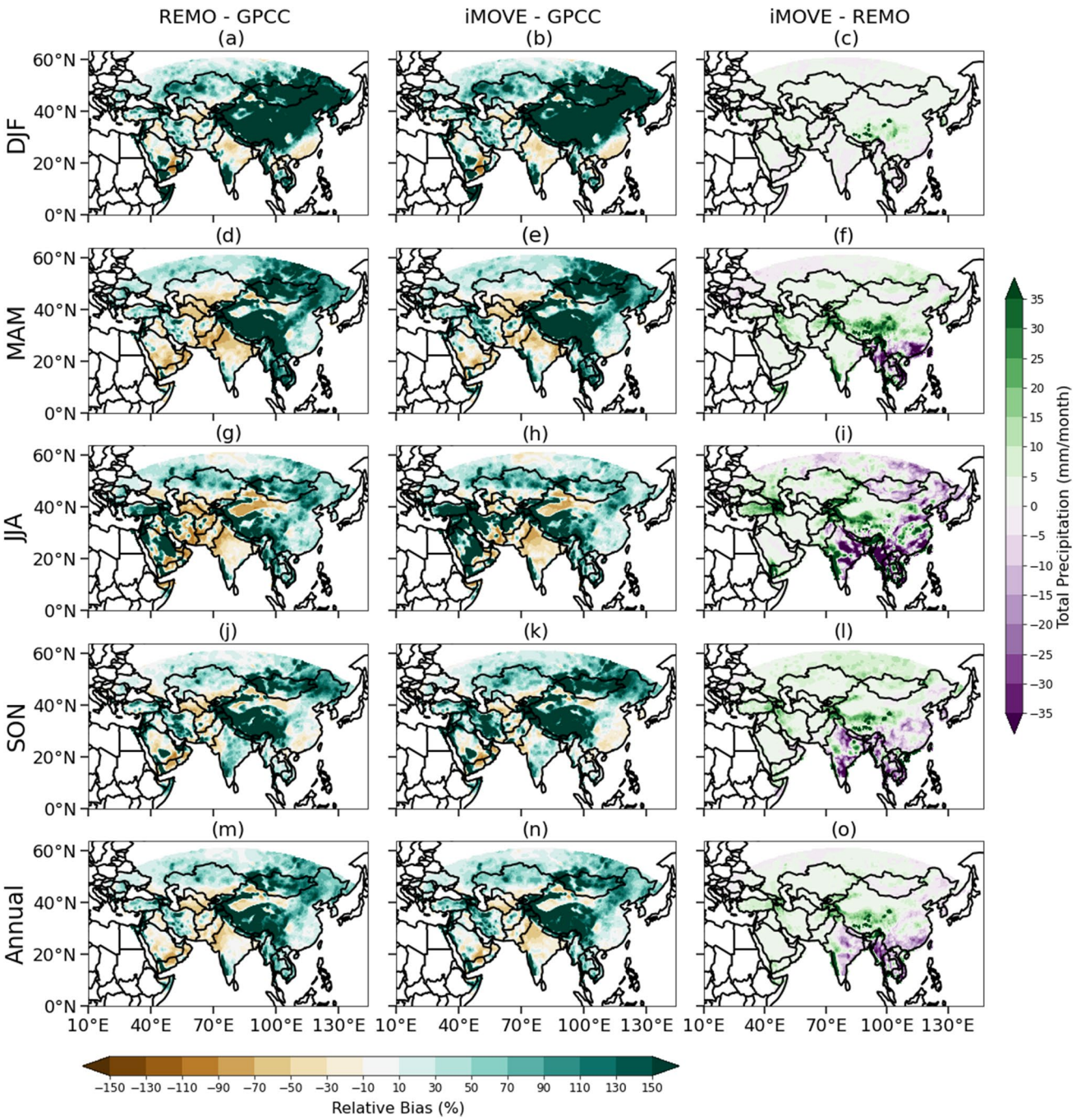

Fig. 4 **a**–**o** Mean monthly total precipitation relative bias (%) at 0.44° for the period 2000–2015. Bias is calculated with respect to GPCC. The last column shows the difference between iMOVE, and standard REMO simulation runs

Table 1 Mean absolute Bias value for total precipitation (mm/month) over CAS-44 (the red box region in Fig. 1) and 0.11° domain

	DJF	MAM	JJA	SON	ANN
REMO_0.44	12.718601	10.974119	11.527166	13.045518	12.066352
iMOVE_0.44	14.024334	14.712525	14.161978	16.911936	14.952696
REMO_0.11	5.174127	4.1128383	2.7613745	3.242991	3.8228328
iMOVE_0.11	5.5818667	5.165372	4.6919956	4.925424	5.0911646

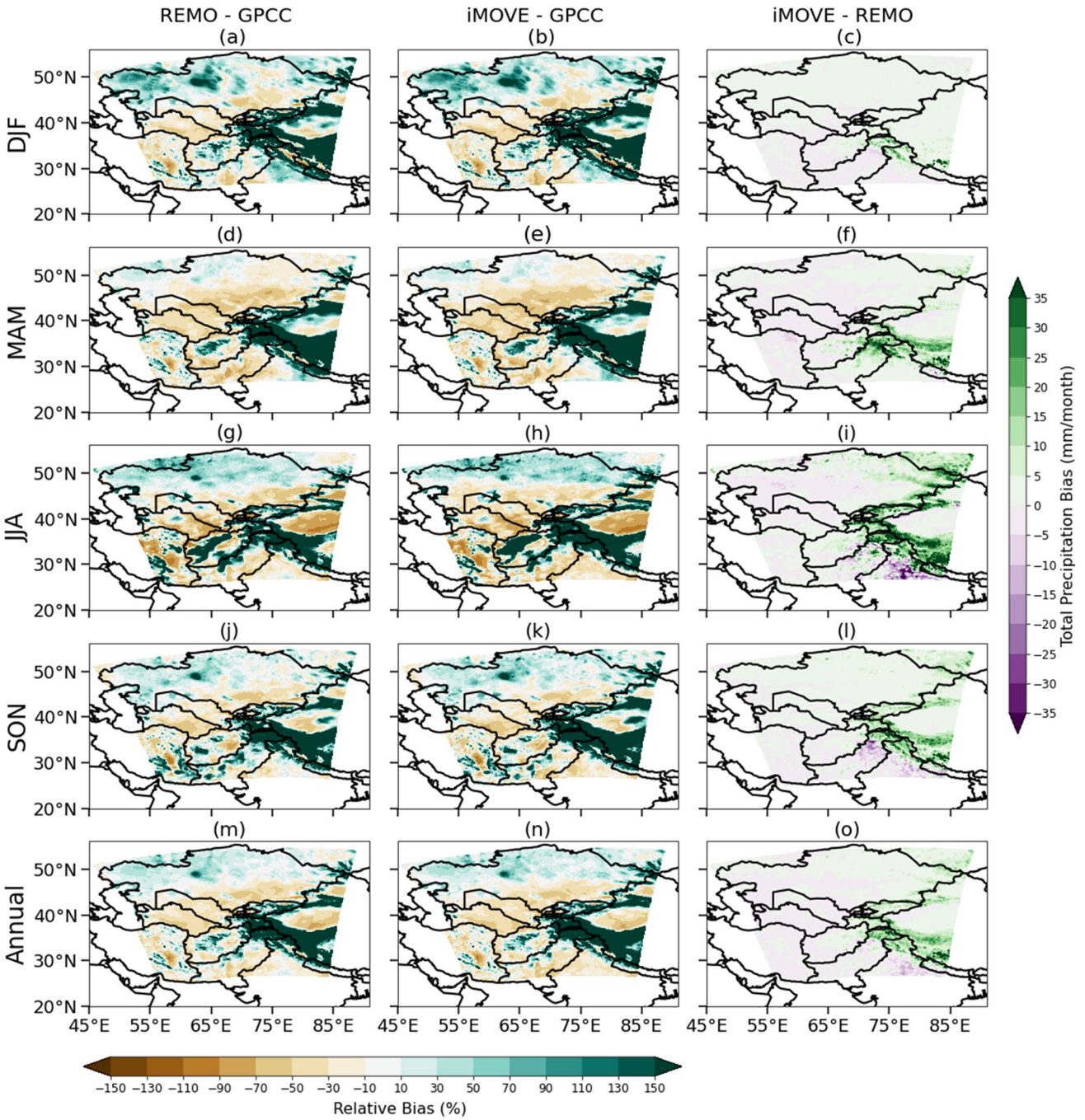

Fig. 5 **a**–**o** Same as Fig. 4, but for 0.11° runs and the bias is calculated with respect to the GPCC

dipole pattern of the biases can be seen on annual time scales with an overestimation in the north and an underestimation in the south of Central Asia (Fig. 5m and n). The difference between iMOVE and REMO (Fig. 5c, f, i, l, and o) demonstrates the higher simulated precipitation in the northern and north-eastern parts of the domain during all seasons. The southern areas are characterized by higher precipitation amounts in REMO. Thus, the bias pattern is enhanced in both directions when interactive vegetation is considered in the model. The absolute bias for 0.11° is shown in Fig. s6 which reveals a lower wet bias during winter which increases in the northern part of the domain as can be seen in Fig. 5.

As mentioned earlier, the larger 0.44° domain is characterized by the presence of various monsoon regions and related with very high precipitation magnitudes in the eastern and southern parts of the domain which come along with

the arid climate of Central Asia. Consequently, a uniform seasonal cycle for this large model domain with different climates is not to be expected which complicates the model validation. Therefore, a principal component analysis (PCA) based on GPCC's precipitation has been performed to identify the major precipitation regions of the domain. For this, the monthly precipitation sum of the study period is considered. These 192 precipitation values act as variables while the number of land grid points in the domain acts as the sample size for the PCA.

The two leading principal components (PCs) explain 40.59% (PC1) and 20.68% (PC2) of the variance, respectively. Figure 6a shows that the patterns of PC1 lie in the monsoon regions. Consequently, this PC represents the summer monsoon precipitation. Contrary to that, PC2 (Fig. 6b) highlights mainly the drier regions of Central Asia, Eastern Europe, and Western Asia and represents precipitation of the winter months. The third and fourth PC (not shown) together explain further 10% of the variance.

The annual cycle of precipitation from REMO and iMOVE is compared with the GPCC for the 0.44° and 0.11° domain and is shown in Fig. 7a and b, respectively. We have also selected a region (red box in Fig. 1a, CAS-44 hereafter) similar to the 0.11° domain to show the effect of increased horizontal resolution. The annual cycle of GPCC (black solid line, Fig. 7a) shows the seasonal evolution of the precipitation with a strong increase from May onwards. This is a clear signal of the monsoon onset. Precipitation reaches its peak during July and afterwards decreases gradually in the following months. This

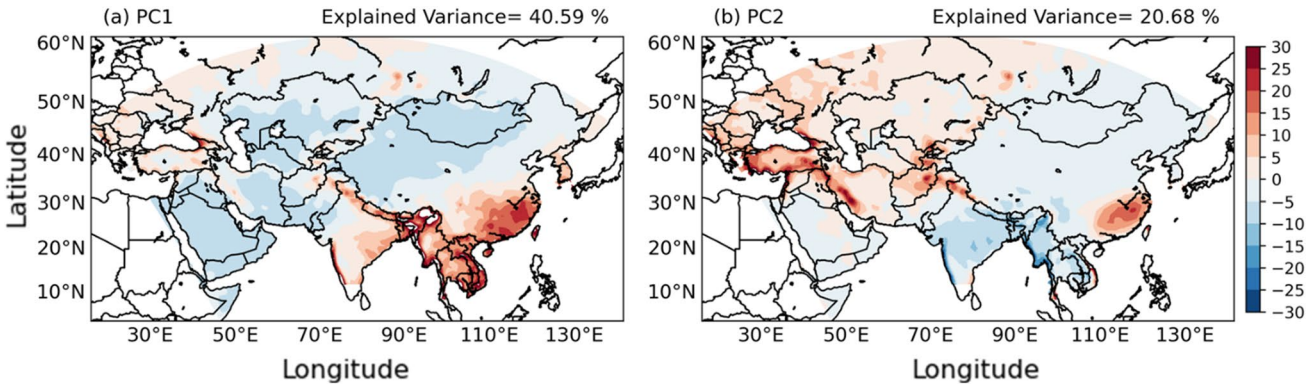

Fig. 6 **a, b** Covariance maps based on principal components (PC1 and PC2) over the 0.44° domain using monthly total precipitation of GPCC observation for the period 2000–2015

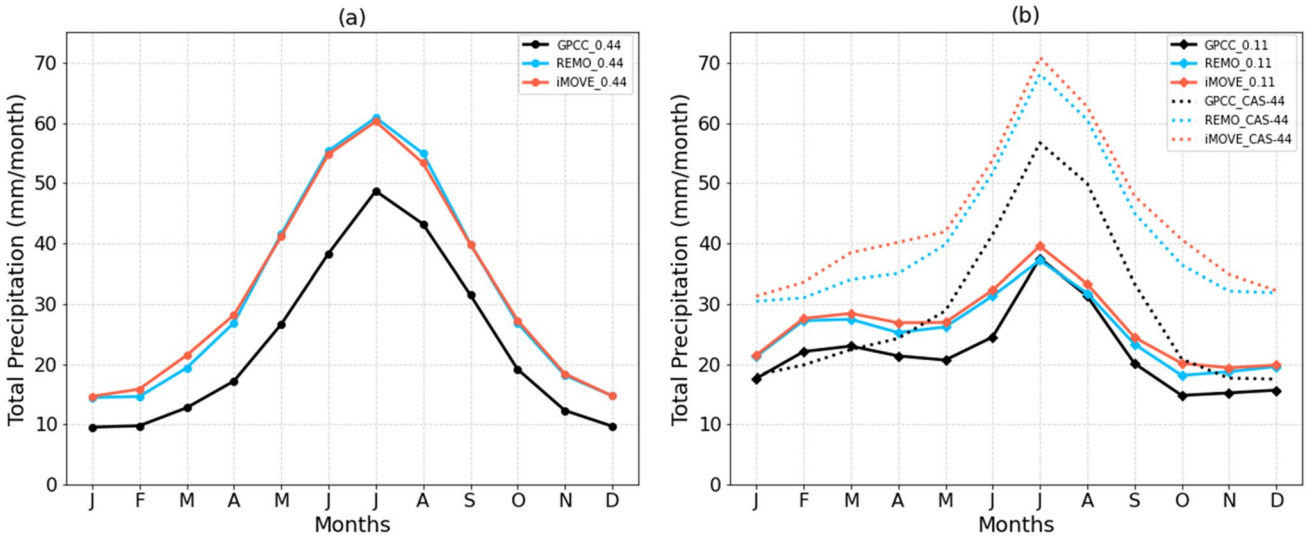

Fig. 7 **a, b** Mean annual cycle of total precipitation of GPCC observation (remapped to respective model domain grids from original 0.25° resolution) and different model experiments averaged over the various model domains i.e. 0.44°, CAS-44, and 0.11° for the period 2000–2015. The dashed lines in **b** represent the CAS-44 region described in Fig. 1

differentiation has already been shown by the PCA. Both, REMO and iMOVE, are able to capture the monthly and seasonal evolution of precipitation, yet with signatures of a strong wet bias during all months. The northern part of the 0.44° domain contributes to the wet bias during the winter months as seen in Fig. 4. As shown earlier, iMOVE tends to produce a slightly higher precipitation bias than REMO. Especially the precipitation during spring is noticeably higher in iMOVE compared to REMO.

The annual cycle at 0.11° resolution shows an improvement in capturing the monthly and seasonal evolution of precipitation for both models with respect to the observations (Fig. 7b). The wet bias in REMO and iMOVE still persists during the winter season but with a lower magnitude. One can observe a decreasing pattern in precipitation magnitude during spring season in GPCC. This is captured well by REMO and iMOVE. The peak precipitation during July and August for REMO almost overlaps with GPCC while iMOVE shows slightly higher precipitation. The comparison of the annual cycle for the CAS-44 region with the 0.11° domain reflects the clear added value of the higher model resolution.

The models' performance is measured by IOA (Willmott 1982). At 0.44° resolution, both, REMO and iMOVE, show a good agreement with observations especially over the Central Asian plains while the orographic regions exhibit a lower value in both simulations (Fig. 8a and b). However, in mountainous regions and the eastern part of the domain, REMO shows slightly higher conformity (0.15–0.35) with observations representing the spatial pattern of precipitation as compared to iMOVE (0.05–0.25). The IOA at 0.11° resolution shows a better agreement between the models and GPCC over the northern and western parts of the domain (Fig. 8c and d). Over the SAM region, a better agreement of REMO at 0.11° resolution in comparison to iMOVE can be observed (Fig. 8c). Interestingly, the areas with lower precipitation amounts like the Central Asian plains and desert regions are captured better by both models, showing the highest degree of agreement irrespective of the model resolution. Vice versa, orographic and monsoon regions have lower degrees of agreement. Precipitation's IOA at 0.11° resolution is in the range of 0.25–0.65 and demonstrates a clear improvement in simulated precipitation compared to the 0.44° resolution. This behaviour has also been found by Prein et al. (2015) who conducted the added value of higher resolutions for precipitation over Europe.

To compare the latitudinal and seasonal variations of monthly precipitation, a Hovmöller plot is presented in Fig. 9. At 0.44° resolution (Fig. 9a, b, and c), one can observe a strong precipitation band in GPCC during summer over the SAM regions (15°N–35°N). This precipitation pattern is captured well by the simulations within a similar latitudinal band but with a higher magnitude, mostly contributed by orographic precipitation, and spread over a longer period (Fig. 9b and c). For Central Asia, both models are in better agreement with the precipitation variability, but the northern part of the domain shows increased precipitation amounts in the models and a higher seasonal variation compared to GPCC. The improved representation of the simulated precipitations' magnitude can be seen at the finer resolution of 0.11° while the higher seasonal variation is still present (Fig. 9d, e, and f). The

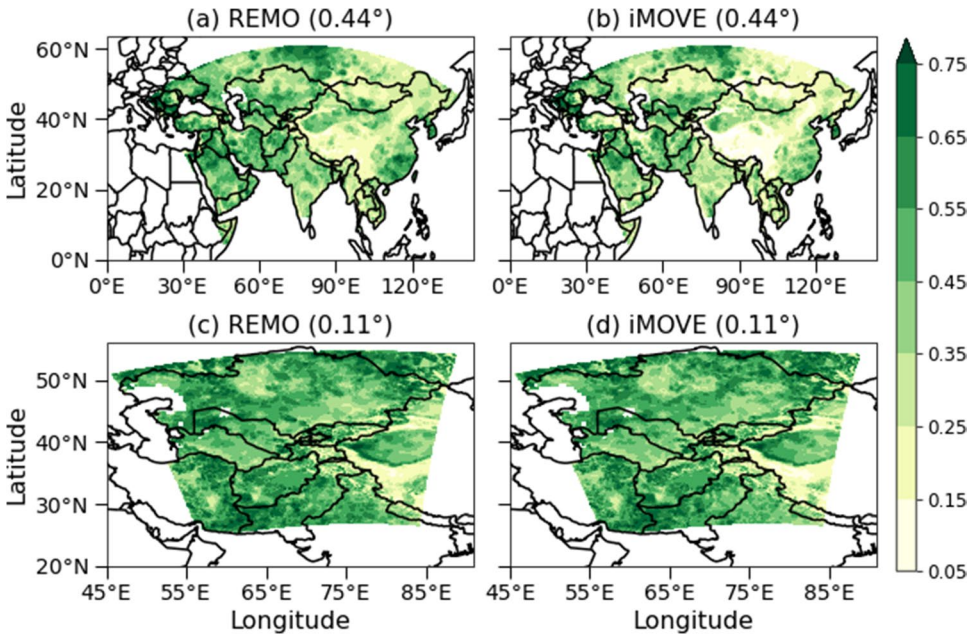

Fig. 8 **a–d** Willmott's Index of Agreement for total precipitation against GPCC for the period 2000–2015 for both model domains and REMO versions

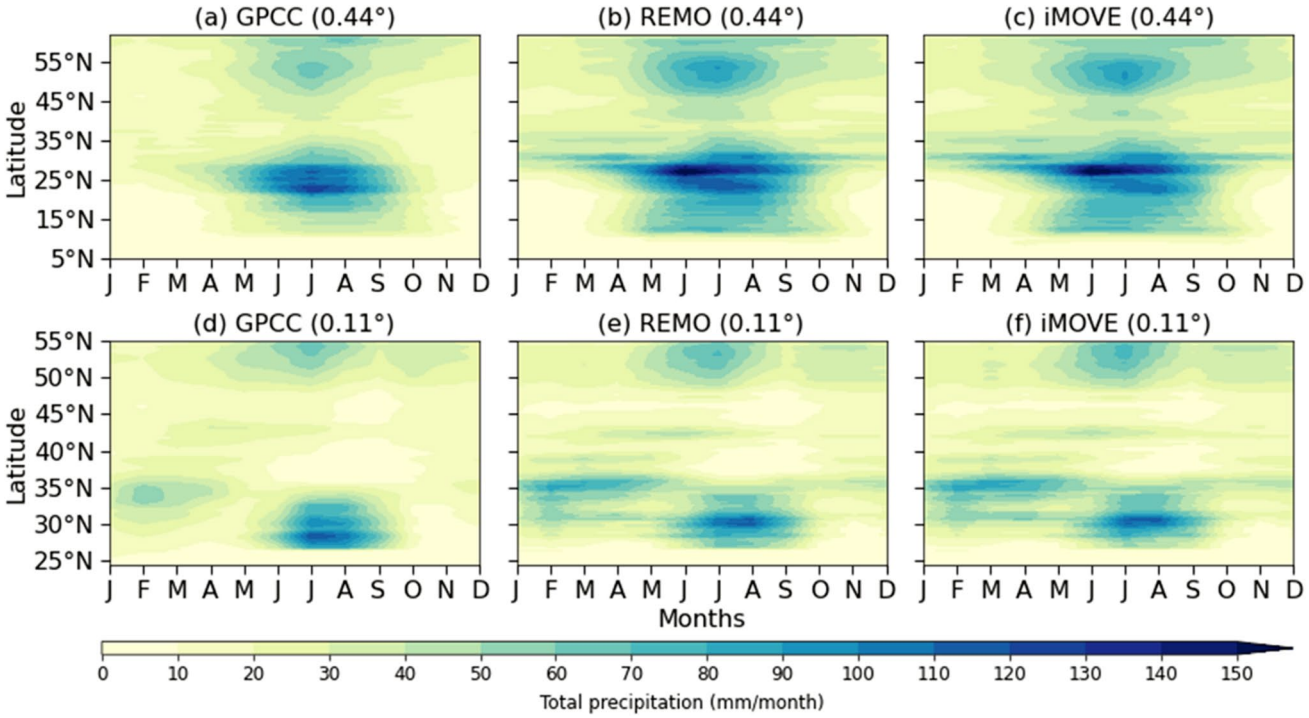

Fig. 9 **a–f** Hovmöller plot showing the latitudinal variation of total precipitation averaged over all longitudes of the model domains (0.44° and 0.11°) for the period 2000–2015

precipitation variability at higher latitudes is more comparable with the magnitude demonstrated by GPCC than at the coarser resolution. A higher amount of precipitation can be observed during winter and spring in REMO and iMOVE at around 30°N in both resolutions.

3.3 Temperature

3.3.1 Mean temperature

We have used ERA5-Land to calculate the monthly 2m mean temperature bias of REMO and iMOVE during different seasons and on an annual scale. The plots are shown in Figs. 10 and 11 for the coarse and the fine resolution, respectively.

On seasonal scales, both models show a substantial warm bias over the eastern part of the domain, especially the Mongolian region, during winter while the Central Asian plains have the lowest magnitude of warm bias (Fig. 10a and b). A similar pattern of warm bias during winter was also reported by Top et al. (2021) while Ozturk et al. (2012, 2016) and Russo et al. (2019) found similar warm bias signatures in the north-eastern part of the domain for RegCM and COSMO-CLM, respectively. Over the Indian region and the south-western part of the domain, iMOVE tends to show a lower warm bias than REMO during the winter season. This becomes more clear when focusing on the difference between iMOVE and REMO in Fig. 10c where REMO tends to show higher temperatures over these regions. A moderate warm bias is present over Central Asia and northern and central India in REMO during spring (Fig. 10d). For iMOVE, the warm bias is lower, especially over the Indian region, and again evident in the difference maps (Fig. 10e and f). During summer, the southern and mountainous regions of Central Asia show a significant warm bias in REMO (Fig. 10g) while the bias magnitude decreases for iMOVE. This is also the case for the northern part of Central Asia and over Pakistan and Afghanistan as demonstrated by the difference plot (Fig. 10h and i). Both models are in good agreement with the validation data during autumn with a better performance of iMOVE (Fig. 10j, k, and l). The models are able to produce an almost identical pattern of mean temperature bias at the annual scale. However, REMO simulates slightly higher temperatures in some parts of the domain (Fig. 10m, n, and o). The slight cold bias at latitudes above 55°N and over some parts of the Tibetan Plateau persists throughout all the seasons and, thus, on the annual scale.

The mean temperature bias at the 0.11° simulations shows an improvement across all seasons (Fig. 11). The seasonal pattern during winter and spring shows a decrease in the warm bias for both simulations especially over the Central Asian plains in comparison to the coarse resolution (Fig. 11a, b, d, and e). For the eastern part, a reduction of the warm bias can also be observed in the finer resolution. Ozturk et al. (2012, 2016) found that the forcing of

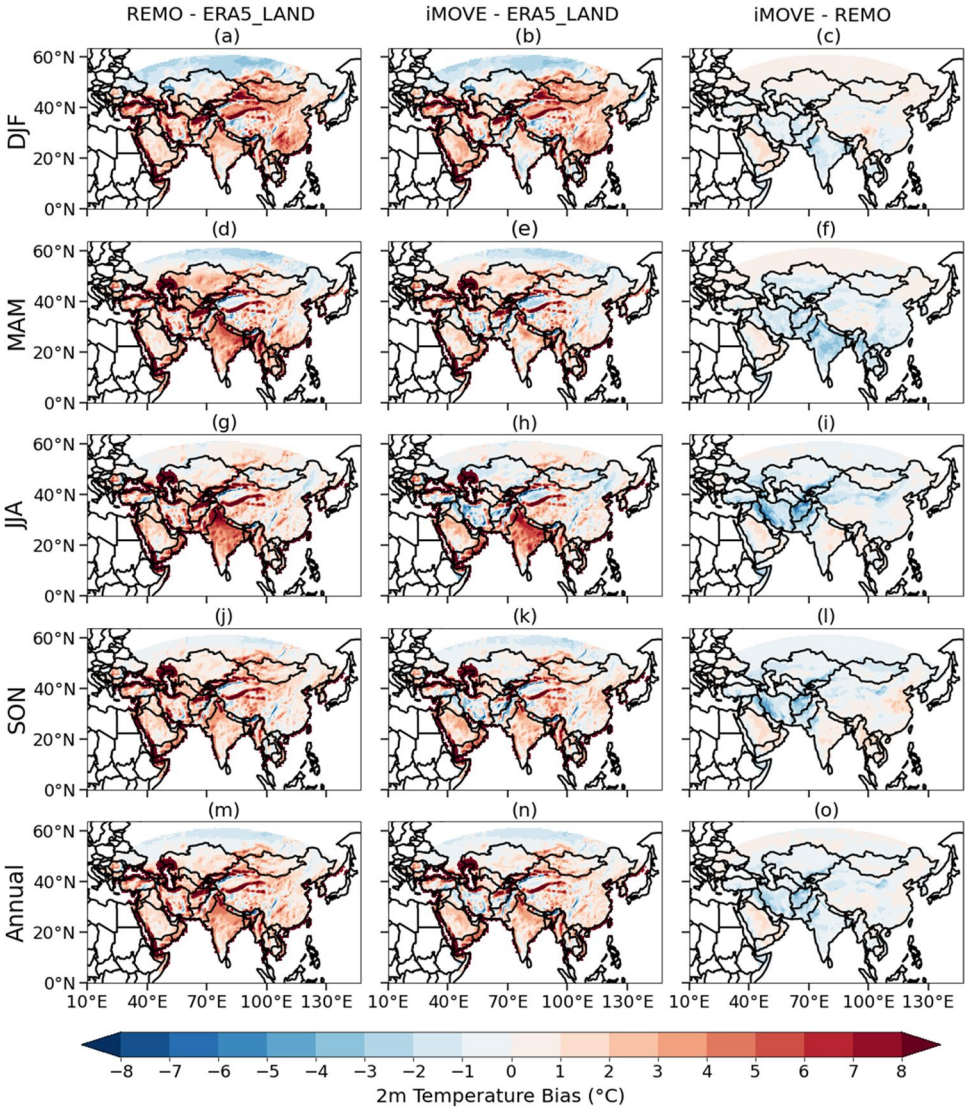

Fig. 10 **a–o** Mean monthly 2m temperature bias (0.44°) for the period 2000–2015. Bias is calculated with respect to ERA5-Land. The last column shows the difference between iMOVE and standard REMO simulation runs

ERA-Interim results in a warm bias in RCMs which occurs also during winter over the northern part of CAS-CORDEX and is related to the inefficiency of ERA-Interim to represent snow cover. In our study, the bias over the orographic regions also shows an improvement due to the higher resolution but the overestimation persists. The slight cold bias in iMOVE during summer and autumn is clearly visible over Central Asia (Fig. 11h and k). Again, the precipitation pattern during autumn is in close agreement with ERA5-Land (Fig. 11j and k). Interestingly, the difference between iMOVE and REMO shows higher temperatures across all seasons in REMO except for winter. Here, iMOVE shows an overestimation in Central Asia (Fig. 11c, f, i, l, and o).

3.3.2 Maximum temperature

The models' biases of the maximum temperature compared to ERA5-Land are presented in Fig. 12 on the annual scale. We show solely the annual maps since the bias patterns of the maximum temperature during the seasons barely differ. At 0.44°, the annual mean biases in maximum temperature are showing a significant underestimation. This is pronounced during summer and autumn, while during winter and spring season, these colder biases have the smallest range especially over the Central Asian part (Fig. s7a, b, d, and e). iMOVE shows a stronger cold bias over orographic regions, especially the Tibetan Plateau (Fig. 12b). On an annual scale, the northern part of the domain is marked by higher maximum temperatures in iMOVE. Vice versa, REMO shows higher values in the southern and south-western parts of the domain (Fig. 12c).

Significant improvements in the maximum temperature can be observed at at 0.11° resolution (Fig. 12d, e, and f). On an annual scale, the cold bias is still present but clearly reduced over the northern and western parts of the domain. A heterogeneous spatial pattern of the maximum

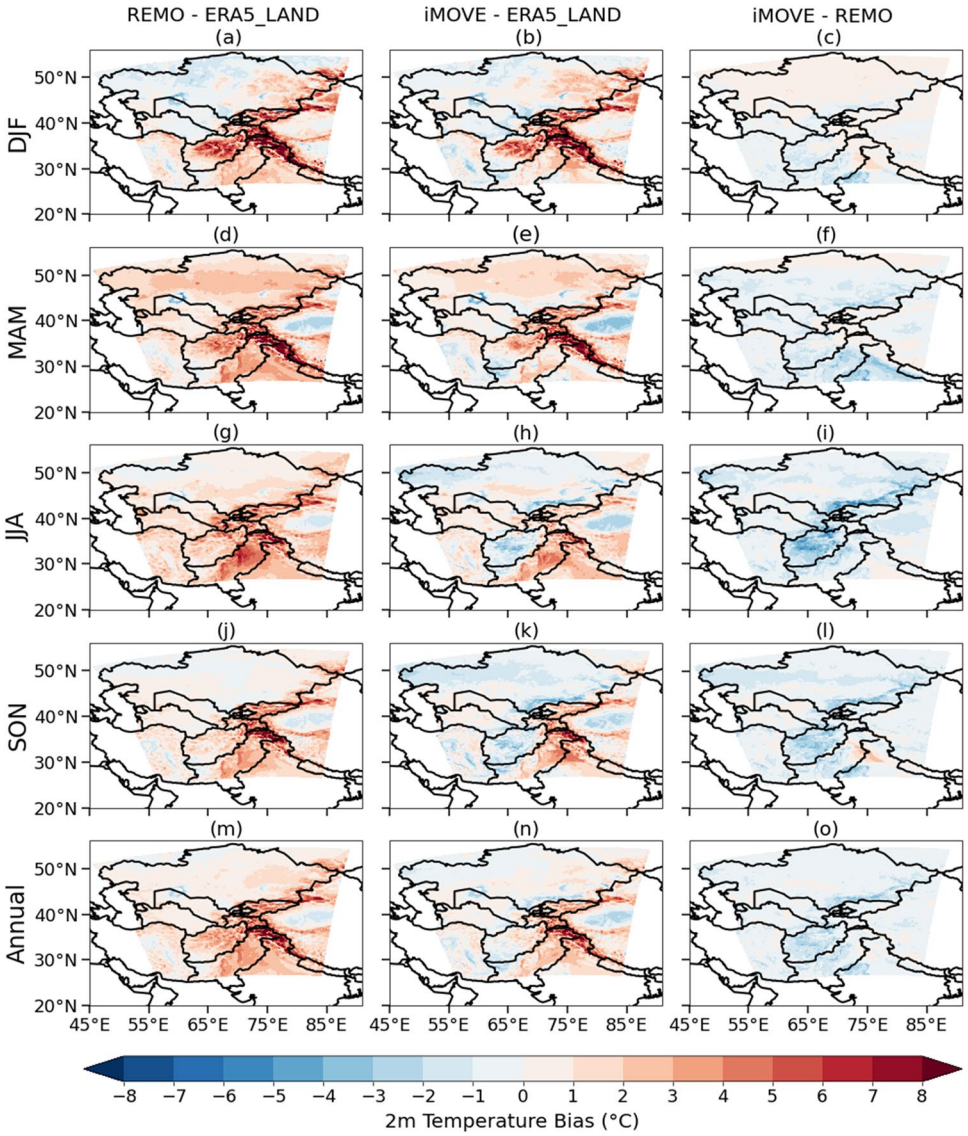

Fig. 11 **a–o** The same as Fig. 12 but for 0.11° runs and the bias is calculated with respect to the ERA5-Land

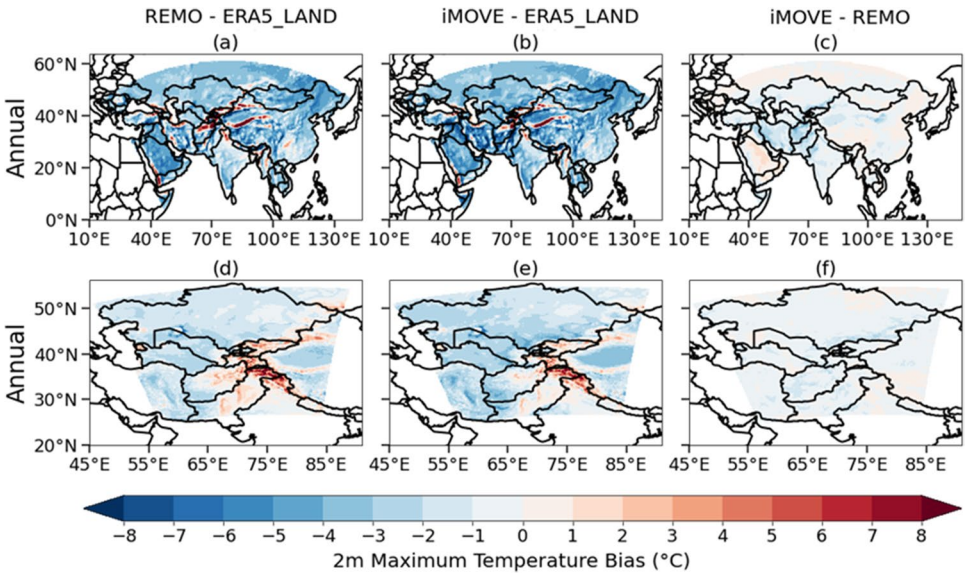

Fig. 12 Mean monthly 2m maximum temperature bias at 0.44° (**a–c**) and at 0.11° (**d–f**) for the period 2000–2015. Bias is calculated with respect to ERA5-Land. The last column shows the difference between iMOVE and standard REMO simulation runs

temperature is present in the difference plot of iMOVE and REMO (Fig. 12f). The temperature's underestimation is again more pronounced in iMOVE during summer and autumn (Fig. s8g, h, j, and k). An overestimation of the maximum temperature, which persists throughout each season and on an annual scale, can be seen over the mountainous region of Kyrgyzstan, Tajikistan, northern part of India and Pakistan. Overall, both models capture the maximum temperature better by applying finer resolution.

3.3.3 Minimum temperature

The spatial bias pattern of the minimum temperature relative to ERA5-Land is presented in Fig. 13 for both resolutions. At 0.44° resolution, the overestimation of the minimum temperature is clearly visible during all the seasons (Fig. s9a-l) and, consequently, also on the annual scale. The bias is present over the entire study area with a relatively high magnitude (Fig. 13a and b). The presence of such a strong warm bias compared to the mean and maximum temperature over the eastern part of the domain, especially the Mongolian region during winter, causes the warm bias in the mean temperature as it was seen in Fig. 10a and b. Interestingly, REMO is simulating higher values of minimum temperature, especially over the southern part of the 0.44° domain whereas iMOVE shows slightly higher values over the Central Asian part (Fig. 13c).

The magnitude of warm biases in minimum temperature reduces significantly at the higher resolution of 0.11° (Fig. 13). The improvement of the warm bias can be seen on an annual scale over Central Asia which is most notable during winter and autumn in both models (Fig. s10a, b, j, and k). The bias patterns during spring and summer show the highest magnitude of bias among all the seasons with a slightly strong warm bias in spring (Fig. s10d, e, g, and h). The magnitude of the biases is slightly lower in iMOVE compared to REMO especially during summer and autumn (Fig. s10g, h, j, and k). Similar to the difference in iMOVE and REMO at 0.44° resolution, the simulated minimum temperature is higher during most of the seasons except winter (Fig. s10c).

The mean annual cycle for the models' simulated mean, maximum, and minimum temperatures along with the data of ERA5-Land at 0.44°, CAS-44, and 0.11° is presented in Fig. 14. For the 2m mean temperature at 0.44°, both models show too high mean temperature during summer and too low mean temperatures during winter months compared to ERA5-Land. However, REMO is closer to the validation data in capturing the mean temperature at 0.44° during summer. Over CAS-44 and 0.11°, both models capture the seasonal variations of the mean temperature well with an improvement at the higher resolution of 0.11° (Fig. 14a and d). Out of both models, iMOVE is closer to the reference dataset, especially at the higher resolution which was also intended by the spatial pattern (Figs. 10 and 11). The seasonal cycle of the maximum temperature shows the inability of both models to capture the seasonal variations (Fig. 14b and e) at a coarser resolution. In contrast, the finer resolution can reproduce the seasonal variation compared to ERA5-Land. Regarding the minimum temperature, iMOVE is closer to the observational and reanalysis data than REMO at both resolutions, while some bias still occurs in both resolutions (Fig. 14c, f, and i). The reduction of that large bias by the usage of iMOVE is an advantage of the new model component.

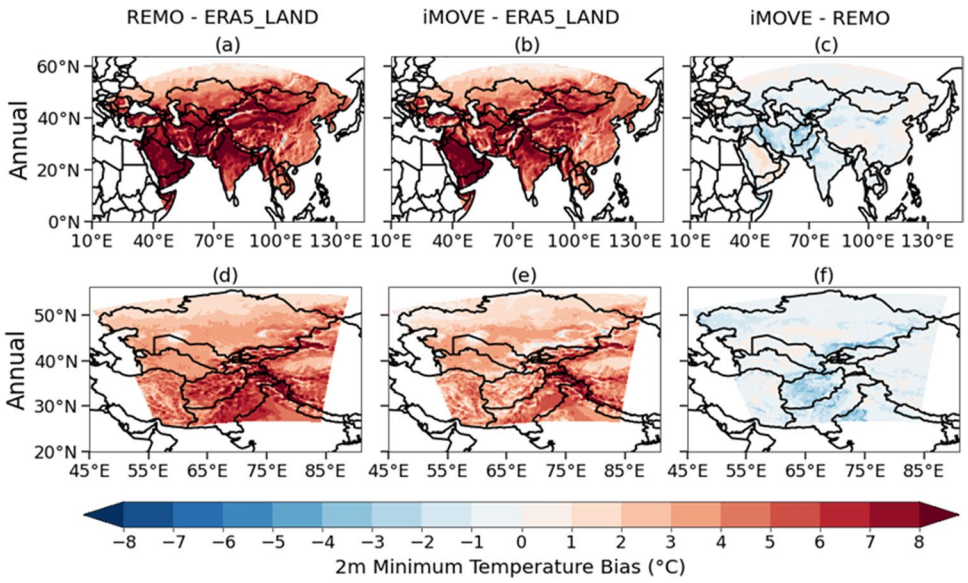

Fig. 13 Mean monthly 2m minimum temperature bias at 0.44° (**a**–**c**) and at 0.11° (**d**–**f**) for the period 2000–2015. Bias is calculated with respect to ERA5-Land. The last column shows the difference between iMOVE and standard REMO simulation runs

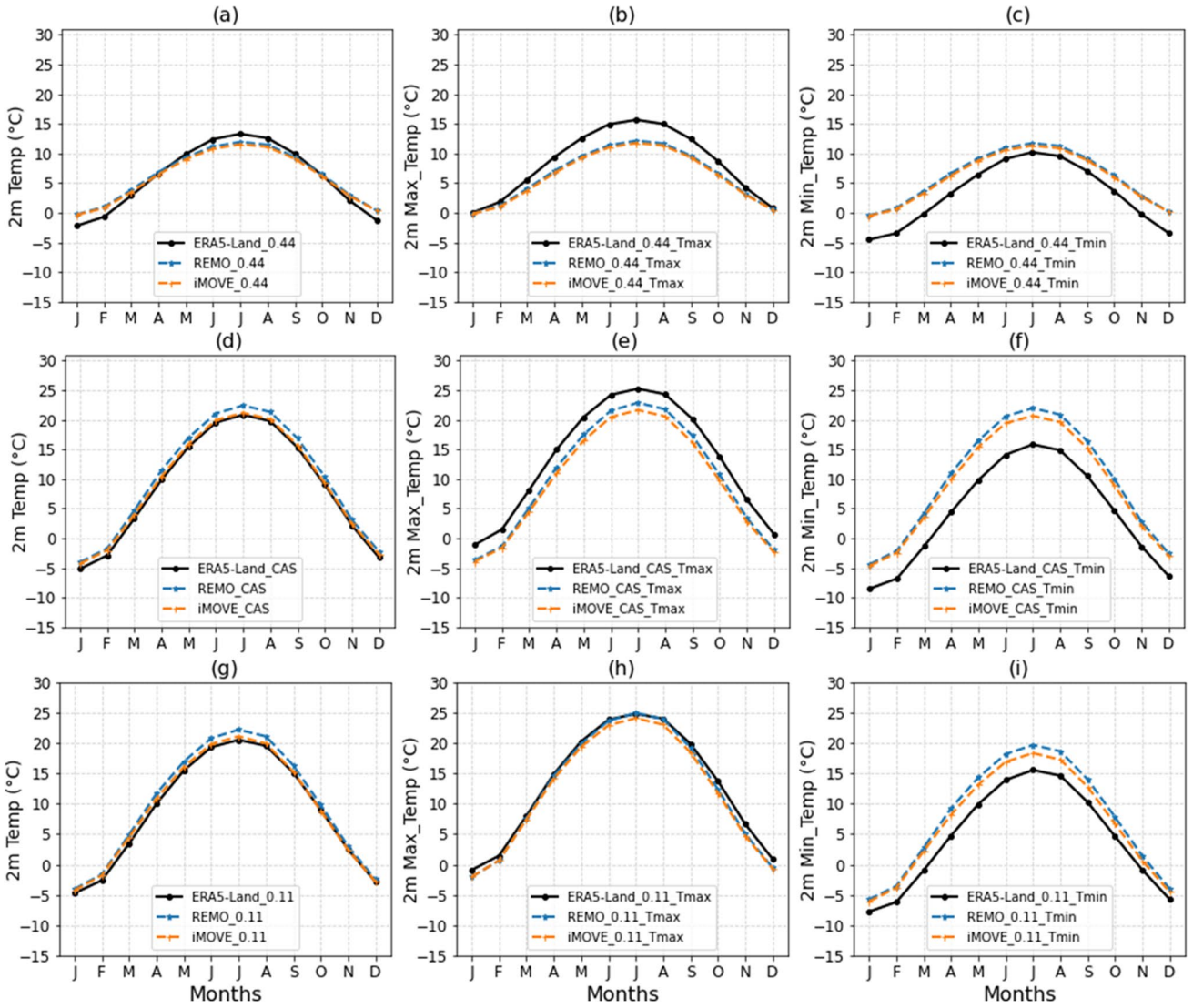

Fig. 14 Mean annual cycle of 2m mean (**a**, **d**), maximum (**b**, **e**), and minimum (**c**, **f**) temperature averaged over the model domains (0.44° and 0.11°) for the period 2000–2015

4 Discussion

4.1 LAI

In the case of vegetation parameters, the behaviour of the LAI was investigated. Using the interactive vegetation which enables this index to show inter-annual variances instead of static values. With the related representation of the vegetation's dependency on atmospheric variables instead of the prescription of inter-annually static values, an important added value is introduced to the simulation. Furthermore, the LAI is generally reduced in the iMOVE-simulations which leads to a systematic improvement compared to AVHRR. The improvement is also demonstrated by the climatological cycle and the difference maps. Additionally, we can state that the combination of LAI and the higher-resolved simulation delivers the best results for this important vegetation index.

Wilhelm et al. (2014) showed that the consideration of iMOVE does not lead to a clear systematic effect on precipitation and temperature in Europe. While, e.g., the prominent cold bias over Russia was reduced for winter and spring, Central Europe, the Mediterranean, and the Balkan showed strong warming for all seasons except winter. The iMOVE version also introduced a dry bias for precipitation over the Balkan during summer and was able to reduce the same bias in autumn. This heterogeneity and complexity are also observed in our study as it is described in detail in the results and the subsequent discussion section. Nevertheless, following Di Luca et al. (2015), it has to be stated that the usage of

iMOVE comes along with an added value since it (i) introduces more and more detailed processes and (ii) improves the representation of vegetation which is directly related to the introduced processes.

4.2 Precipitation

Observed gridded precipitation datasets' accuracy decreases in mountainous regions with elevation, especially above 1500 m (Zhu et al. 2015). Additionally, they underestimate solid precipitation (Palazzi et al. 2013; Sun et al. 2018). The strong wet bias and, hence, the overestimated precipitation in both REMO and iMOVE on seasonal and annual scales over the mountains of Central Asia and the Tibetan Plateau is in accordance with the study by Zhu et al. (2015) because of the mentioned underestimation by gridded precipitation data. Similar patterns of large wet biases over the Tibetan Plateau using COSMO-CLM were also reported in the study of Russo et al. (2019). This wet bias, which is common for several RCMs in regions with complex orography (Gao et al. 2015; Guo et al. 2018), is possibly coming from inaccurately simulated planetary boundary layer (Xu et al. 2016) and/or enhanced orographic precipitation estimation in the models (Gerber et al. 2018). The presented bias patterns of precipitation across different seasons and on the annual scale were also reported by Ozturk et al. (2012; 2016), Russo et al. (2019), and Top et al. (2021), using RCM simulations at resolutions of 0.50°and 0.22°, respectively. The behaviour of the simulated precipitation, especially at the resolution of 0.11° as shown in Fig. 5 and the overestimation of precipitation over the orographic regions and in the eastern part of the domain during most seasons and on the annual scale, is comparable with their findings. Furthermore, the dry bias observed mostly over the north-western and SAM region, which is most prevalent during summer, is also reported in the mentioned studies. A possible mechanism for biases in precipitation is explained by Ozturk et al. (2012). The authors observed a decreased precipitation during summer because of lower regional temperatures and thus weakened pressure gradients over the region. In our study, both models are in accordance with the observations in capturing the precipitation variability, especially at the higher resolution, which has a better representation of the spatial heterogeneity. The effect of orography and land cover, which affects the temperature more systematically than precipitation, is one of the reasons for the lower accuracy of simulated precipitation (Kotlarski et al. 2014). Additionally, in order to improve the precipitation evaluation, it is important to reduce the uncertainty range and error in the gridded observational products (Russo et al. 2019). Mannig et al. (2013) also reported lower precipitation biases at finer resolution in REMO in comparison to the coarsely resolved simulations. They argued that the inefficiency in simulating precipitation does not necessarily arise from bad parametrization but from a poor representation of land surface properties which are especially important in the southern part of Central Asia where irrigation and land cover have a strong impact on precipitation (Lioubimtseva et al. 2005). Furthermore, the inability of REMO to reproduce the mean annual cycle, especially over the Asian monsoon region, is also reported in the study of Top et al. (2021). Similarly, over the subtropical regions, which are influenced by the Asian monsoon system, Remedio et al. (2019) also observed a wet bias on the annual timescale.

4.3 Temperature

Overall, REMO and iMOVE capture the mean temperature variability and annual cycle well at 0.44° and show significant improvements at higher resolution of 0.11° (Figs. 10, 11, and 14). Additionally, regarding the biases, the models are in a comparable range with other RCMs from CORDEX-CAS following the studies from Ozturk et al. (2012, 2016), Russo et al. (2019), and Top et al. (2021) and over the sub-region of Central Asia (Wang et al. 2020; Zhu et al. 2020). The highest agreement between models and reference datasets for mean temperature was observed during autumn, while warm biases are strongest during spring and winter with a better performance of the finer resolution (Figs. 10 and 11). The strong warm bias (> 5 °C) during winter over Mongolia and the north-eastern part of the domain at 0.44° was also observed in the studies of Ozturk et al. (2012, 2016) and Top et al. (2021). Ozturk et al. (2012, 2016) concluded that it emerges from the driving ERA-Interim data which has a warm bias over this part of the domain due to its inability to simulate the snow cover adequately. Top et al. (2021) also concluded that the warm bias in the eastern part of the 0.44° domain is caused by the warm forcing data. Additionally, CRU has a tendency to show a cold temperature bias over Russia in winter (New et al. 1999). Note that our 0.11° domain is not extended northward as it is in Top et al. (2021) for their 0.22° resolution.

The cold bias during spring in the north-eastern part of the 0.44° domain was also reported by Ozturk et al. (2012, 2016) for their 0.50° run and by Top et al. (2021). All studies attributed this to the fact that either snow-related processes are simulated incorrectly by the models or the occurrence of snow cover is delayed. However, Russo et al. (2019) did not observe a significant reduction of warm bias over the north-eastern part of their domain after changing the snow scheme in COSMO-CLM. Ozturk et al. (2012) obtained significantly improved temperature patterns in the north of CORDEX-CAS after the use of a cloud correction scheme in RegCM. Thus, the

simulated total cloud cover can be another possible explanation for the temperature bias in the northern part of the domain. During summer, a weak cold bias in the north of the domain and the warm bias in the south of the 0.44° simulation as well as a similar but more pronounced bias pattern at 0.11° resolution is observed. This is coherent with the findings from Russo et al. (2019) and Top et al. (2021). They also observed a similar bias pattern except for some areas on the Tibetan Plateau region for COSMO-CLM.

For maximum and minimum temperatures of the coarse resolution, strong cold and warm biases were observed, respectively (Figs. 12 and 13). Both, REMO and iMOVE, underestimate the maximum temperature and overestimate the minimum temperature which is also quite evident from their annual cycle, and hence, it shows the models' inability to capture the diurnal temperature range (Fig. 14b and c). Yet, iMOVE tends to reduce that bias. The respective cold and warm biases in maximum and minimum temperatures were also present in the higher resolved simulations but with substantially reduced magnitude compared to the 0.44° simulation (Figs. 12 and 13). This suggests that increasing the horizontal resolution of RCMs is an effective way to reduce the magnitude of biases. Studies by Laprise et al. (2003) and Kyselý and Plavcová (2012) over different regions and by Russo et al. (2019) and Top et al. (2021) over the CORDEX-CAS domain also found the underestimation in the diurnal range within different RCMs. Thus, this seems to be a general weakness of RCMs that can be effectively reduced by the interactive vegetation which is a clear added value. The cold bias pattern in high orographic regions, especially over the Tibetan Plateau and the Himalayas, may be primarily due to the gridded observations which are less reliable in these regions (Russo et al. 2019).

Generally, it can be said that there are some shortcomings of regional climate modeling independent of the target resolution (e.g., Lucas-Picher et al. 2021 and studies cited in there). On the one hand, the results of an RCM depend on the boundary forcing data provided by a reanalysis (in our case ERA-Interim) or a GCM. Thus, if the boundary forcing shows systematic errors, the RCM might show a higher resolved representation of those as well—depending on the domain size and setting (Laprise et al. 2008). Additionally, excluding convection-permitting simulations, an RCM—like in present simulations—uses the same parameterization schemes to discretize processes smaller than the simulated grid. With this, a systematic error can occur depending, e.g., on the examined season or region. In the present work, soil hydrological processes are barely represented which is influencing the energy fluxes between the land surface and the atmosphere and has already been a point of critique in Wilhelm et al. (2014). This is tackled in currently ongoing work by the introduction of a multilayer soil scheme and the consideration of irrigation.

5 Summary and conclusion

In the present study, the evaluation of RCM simulations over Central Asia at the horizontal resolution of 0.44° and 0.11° has been carried out. The regional climate model REMO (v2015) and its vegetation-coupled version REMO-iMOVE, which is used for the first time out of Europe, have been considered. Both model versions are generally able to capture the precipitation variability very well at the finer resolution of 0.11° with a relatively higher magnitude of simulated precipitation in iMOVE, especially in northern and north-eastern parts of the domain. A wet bias during winter and summer and a dry bias in spring over northern Central Asia were found in both models. Over high-elevated regions, mainly the Tibetan Plateau and Himalayas, erroneous precipitation was observed at both resolutions. Both models are also able to capture the seasonal cycle of precipitation, with REMO performing relatively better, especially during summer at 0.11° resolution. The best performance from both versions is observed in autumn where precipitation biases are within the observational uncertainty at both resolutions.

In terms of mean temperature, a warm bias in the north-eastern part of the domain occurs during the winter season at both resolutions, which probably arises from the driving ERA-Interim data (Ozturk et al. 2012, 2016) and inaccurate simulation of snow cover (Russo et al. 2019; Top et al. 2021). Regarding the temperature extremes, the underestimation of maximum and overestimation of minimum temperature, respectively, results in an inaccurate simulation of the diurnal temperature range which becomes visible in the investigated monthly values as well. At the higher resolution of 0.11°, this aspect is clearly improved compared to the coarser resolution. Again, the lowest bias of temperature is also observed during autumn for both versions. There is a need to consider more variables to get a more thorough picture of the added value of the high resolution instead of only analysing precipitation and temperature.

Overall, the vegetation-coupled version iMOVE performs quite similarly to its parent version REMO in capturing the mean climate over the Central Asian region. As the biases in temperature are reduced but still being present in iMOVE, this indicates the involvement of other processes apart from surface variables (Wilhelm et al. 2014). According to them, major differences in

near-surface climate between iMOVE and REMO can be restricted to some regions and are mostly related to the new representation of vegetation phenology. Furthermore, Wilhelm et al. (2014) attributed the differences in REMO and iMOVE to the different temporal dynamics of vegetation cover and density and changes in the soil scheme. The moisture and surface heat flux gets affected by these parameters leading to a modification in the simulated near-surface climate. Indeed, the representation of the LAI shows a clear improvement in inter-annual variability and magnitude for both domains and in seasonal cycle and spatial patterns for Central Asia.

In summary, the finer resolved simulations at 0.11° of both REMO versions represent the spatial details in climate variables much better and can be used for climate impact studies and future climate change projections. The coupled iMOVE version is able to simulate the temperature patterns better in comparison to REMO, especially at a higher resolution. However, the main point of iMOVE is the clear improvement of LAI's simulation by implementing an interactive instead of a static and, thus, more complex vegetation scheme. Thus, an added value is achieved (Di Luca et al. 2015).

Further studies are required in the future to analyse the cloud cover and snow-related processes in detail at a finer resolution to better understand the bias patterns in precipitation and temperature. We recommend the usage of iMOVE in future studies due to its clear advantage in reproducing the diurnal temperature range and the annual cycle of LAI, e.g., to examine vegetation dynamics and land use and land cover changes and their effects on local and regional climate dynamics in Central Asia. Additionally, we follow the recommendation of Wilhelm et al. (2014) to combine iMOVE with a multilayer soil scheme and undertake that task for upcoming studies. A subsequent step can be the coupling to dynamic vegetation schemes which are able to change the plant functional types depending on long-term changing climate conditions. It has been shown that the consideration of these models adds value to the climate models and creates new research opportunities (Rachmayani et al. 2015; Shi et al. 2018; Drüke et al. 2021; Zhang et al. 2022).

Supplementary Information The online version contains supplementary material available at https://doi.org/10.1007/s00704-022-04233-y.

Acknowledgements We thank the ECMWF for producing and making available the ERA-Interim and ERA5-Land re-analyses. The precipitation variable from the GPCC dataset has kindly been provided via the webpage https://opendata.dwd.de/climate_environment/GPCC/html/fulldatamonthly_v2018_doi_download.html.

Author contribution HP and PR conceptualized the idea. PR, KZ, DA, and FP contributed to the model development and experimental setup. PR wrote the main manuscript and prepared figures with help of KZ and DA. All authors reviewed the manuscript and contributed to the final version. HP was responsible for funding acquisition.

Funding Open Access funding enabled and organized by Projekt DEAL. This work was funded by the German Research Foundation under grant PA 1194/17–1 (AOBJ: 660612).

Data availability Data will be available upon request from the corresponding author (praveen-kumar.rai@uni-wuerzburg.de).

Code availability The open-source Python codes have been used in the present study for analysis purpose. The code for findings will be available from the corresponding author (praveen-kumar.rai@uni-wuerzburg.de).

Declarations

Competing interests The authors declare no competing interests.

Ethics approval It is not necessary.

Consent to participate All authors approved.

Consent for publication The authors give their consent to the publication of all details of the manuscript, including texts, figures, and tables.

References

Aizen VB, Aizen EM, Kuzmichonok VA (2007) Glaciers and hydrological changes in the Tien Shan: simulation and prediction. Environ Res Lett 2:045019

Asner GP, Braswell BH, Schimel DS, Wessman CA (1998) Ecological research needs from multiangle remote sensing data. Remote Sens Environ 63:155–165

Bartholome E, Belward A (2005) GLC2000: A new approach to global land cover mapping from Earth observation data. Int J Remote Sens 26–9:1959–1977

Breil M, Rechid D, Davin EL, de Noblet-Ducoudré N, Katragkou E et al (2020) The opposing effects of re/af-forestation on the diurnal temperature cycle at the surface and in the lowest atmospheric model level in the European summer. J Clim 33:9159–9179. https://doi.org/10.1175/JCLI-D-19-0624.1

Chan SC, Kendon EJ, Fowler HJ, Blenkinsop S, Ferro CAT, Stephenson DB (2013) Does increasing the spatial resolution of a regional climate model improve the simulated daily precipitation? Clim Dyn 41(5–6):1475–1495. https://doi.org/10.1007/s00382-012-1568-9

Chevallier P, Pouyaud B, Mojaïsky M, Bolgov M, Olsson O, Bauer M, Froebrich J (2014) River flow regime and snow cover of the

Pamir Alay (Central Asia) in a changing climate. Hydrol Sci J 59(8):1491–1506
Davin EL, Rechid D, Breil M, Cardoso RM, Coppola E, Hoffmann P, Jach LL, Katragkou E, de Noblet-Ducoudré N, Radtke K, Raffa M, Soares PMM, Sofiadis G, Strada S, Strandberg G, Tölle MH, Warrach-Sagi K, Wulfmeyer V (2020) Biogeophysical impacts of forestation in Europe: first results from the LUCAS Regional Climate Model intercomparison. Earth Syst Dyn 11:183–200. https://doi.org/10.5194/esd-11-183-2020
Dee DP, Uppala SM, Simmons AJ, Berrisford P, Poli P et al (2011) The ERA-Interim reanalysis: configuration and performance of the data assimilation system. Q J Roy Meteor Soc 137:553–597. https://doi.org/10.1002/qj.828
Di Luca A, de Elía R, Laprise R (2015) Challenges in the quest for added value of regional climate dynamical downscaling. Curr Clim Chang Rep 1(1):10–21
Drüke M, von Bloh W, Petri S, Sakschewski B, Schaphoff S, Forkel M, Huiskamp W, Feulner G, Thonicke K (2021) CM2Mc-LPJmL v.1 0: Biophysical coupling of a process-based dynamic vegetation model with managed land to a general circulation model. Geosci Model Dev 14(6):4117–4141
Duishonakunov M, Imbery S, Narama C, Mohanty A, King L (2014) Recent glacier changes and their impact on water resources in Chon and Kichi Naryn Catchments, Kyrgyz Republic. Water Science and Technology: Water Supply 14(3):444–452
Fischer G, Shah MN, Tubiello F, Van Velhuizen H (2005) Socio-economic and climate change impacts on agriculture: an integrated assessment, 1990–2080. Philosophical Transactions of the Royal Society b: Biological Sciences 360(1463):2067–2083
Fu C, Wang S, Xiong Z, Gutowski WJ et al (2005) Regional climate model intercomparison project for Asia (RMIP). Bull Am Meteorol Soc 86(2):257–266
Gao Y, Xu J, Chen D (2015) Evaluation of WRF mesoscale climate simulations over the Tibetan Plateau during 1979–2011. J. Climate 28:2823–2841
Gerber F, Besic N, Sharma V, Mott R, Daniels M, Gabella M, Berne A, Germann U, Lehning M (2018) Spatial variability in snow precipitation and accumulation in COSMO–WRF simulations and radar estimations over complex terrain. Cryosphere 12:3137–3160. https://doi.org/10.5194/tc-12-3137-2018,a
Gessner U, Naeimi V, Klein I, Kuenzer C, Klein D, Dech S (2013) The relationship between precipitation anomalies and satellite-derived vegetation activity in Central Asia. Glob Planet Chang 110:74–87
Gibson PB, Waliser DE, Lee H, Tian B, Massoud E (2019) Climate model evaluation in the presence of observational uncertainty: precipitation indices over the Contiguous United States. J Hydrometeorol 20:1339–1357
Giorgi F (2019) Thirty years of regional climate modeling: where are we and where are we going next? Journal of Geophysical Research: Atmospheres 124(11):5696–5723. https://doi.org/10.1029/2018JD030094
Giorgi F, Gao XJ (2018) Regional Earth system modeling: review and future directions. Atmos Ocean Sci Lett 11:189–197
Giorgi F, Coppola E, Teichmann C, Jacob D (2021) Editorial for the CORDEX-CORE experiment I special issue. Clim Dyn 57:1265–1268. https://doi.org/10.1007/s00382-021-05902-w
Giorgio F, Mearns LO (1999) Introduction to special section: regional climate modeling revisited. J Geophys Res 104:6335–6352. https://doi.org/10.1029/98JD02072
Giot O, Termonia P, Degrauwe D, De Troch R, Caluwaerts S, Smet G, Berckmans J, Deckmyn A, De Cruz L, De Meutter P, Duerinckx A, Gerard L, Hamdi R, Van den Bergh J, Van Ginderachter M, Van Schaeybroeck B (2016) Validation of the ALARO-0 model within the EURO-CORDEX framework. Geosci Model Dev 9:1143–1152. https://doi.org/10.5194/gmd-9-1143-2016
Guo D, Sun J, Yu E (2018) Evaluation of CORDEX regional climate models in simulating temperature and precipitation over the Tibetan Plateau. Atmospheric and Oceanic Science Letters 11:219–227. https://doi.org/10.1080/16742834.2018.1451725a,b
Hagemann S (2002) An improved land surface parameter data set for global and regional climate models, Max Planck Institute for Meteorology report series, Report No. 336, Hamburg, Germany
Hagg W, Braun LN, Kuhn M, Nesgaard TI (2007) Modelling of hydrological response to climate change in glacierized Central Asian catchments. J Hydrol 332(1–2):40–53
Harris I, Osborn TJ, Jones PD, Lister DH (2020) Version 4 of the CRU TS monthly high-resolution gridded multivariate climate dataset. Scientific Data 7:1–18. https://doi.org/10.1038/s41597-020-0453-3
Hofstra N, New M, McSweeney C (2010) The influence of interpolation and station network density on the distributions and trends of climate variables in gridded daily data. Clim Dyn 35:841–858. https://doi.org/10.1007/s00382-009-0698-1
Holdridge LR (1967) Life zone ecology. Life zone ecology., (rev. ed.))
Hu Z, Zhou Q, Chen X, Li J, Li Q, Chen D, Liu W, Yin G (2018) Evaluation of three global gridded precipitation data sets in central Asia based on rain gauge observations. Int J Climatol 38:3475–3493. https://doi.org/10.1002/joc.5510
Huang X, Oberhänsli H, von Suchodoletz H, Prasad S, Sorrel P, Plessen B et al (2014) Hydrological changes in western Central Asia (Kyrgyzstan) during the Holocene as inferred from a palaeolimnological study in lake Son Kul. Quatern Sci Rev 103:134–152
Jacob D (2001) A note to the simulation of the annual and inter-annual variability of the water budget over the Baltic Sea drainage basin. Meteorol Atmos Phys 77:61–73. https://doi.org/10.1007/s007030170017
Jacob D, Podzun R (1997) Sensitivity studies with the regional climate model REMO. Meteorol Atmos Phys 63:119–129. https://doi.org/10.1007/BF01025368
Jacob D, Elizalde A, Haensler A, Hagemann S, Kumar P, Podzun R, Rechid D, Remedio AR, Saeed F, Sieck K, Teichmann C, Wilhelm C (2012) Assessing the transferability of the regional climate model REMO to different coordinated regional climate downscaling experiment (CORDEX) regions. Atmosphere 3:181–199. https://doi.org/10.3390/atmos3010181
Jarlan L, Balsamo G, Lafont S, Beljaars A, Calvet JC, Mougin E (2008) Analysis of leaf area index in the ECMWF land surface model and impact on latent heat and carbon fluxes: application to West Africa. J Geophys Res D: Atmos 113(24). https://doi.org/10.1029/2007JD009370 (art. no. D24117)
Kenzhebaev R, Barandun M, Kronenberg M, Chen Y, Usubaliev R, Hoelzle M (2017) Mass balance observations and reconstruction for Batysh Sook Glacier, Tien Shan, from 2004 to 2016. Cold Reg Sci Technol 135:76–89
Kotlarski S (2007) A subgrid glacier parameterisation for use in regional climate modelling, PhD thesis, Max Planck Institute for Meteorology, Hamburg, Germany, Reports on Earth System Science, No. 42
Kotlarski S, Keuler K, Christensen OB, Colette A, Déqué M, Gobiet A, Goergen K, Jacob D, Lüthi D, van Meijgaard E, Nikulin G, Schär C, Teichmann C, Vautard R, Warrach-Sagi K, Wulfmeyer V (2014) Regional climate modeling on European scales: a joint standard evaluation of the EURO-CORDEX RCM ensemble. Geosci Model Dev 7:1297–1333. https://doi.org/10.5194/gmd-7-1297-2014
Kotova L, Aniskevich S, Bobylev L, Caluwaerts S, De Cruz L, De Troch R, Gnatiuk N, Gobin A, Hamdi R, Sakalli A, Sirin A, Termonia P, Top S, Van Schaeybroeck B, Viksna A (2018) A new project AFTER investigates the impacts of climate change in the Europe-Russia-Turkey region. Clim Serv 12:64–66. https://doi.org/10.1016/j.cliser.2018.11.003

Kumar D, Rai P, Dimri AP (2020) Investigating Indian summer monsoon in coupled regional land–atmosphere downscaling experiments using RegCM4. Clim Dyn 54(5):2959–2980

Kyselý J, Plavcová E (2012) Biases in the diurnal temperature range in Central Europe in an ensemble of regional climate models and their possible causes. Clim Dynam 39:1275–1286. https://doi.org/10.1007/s00382-011-1200-4

Laprise R, Caya D, Frigon A, Paquin D (2003) Current and perturbed climate as simulated by the second-generation Canadian Regional Climate Model (CRCM-II) over northwestern North America. Clim Dynam 21:405–421. https://doi.org/10.1007/s00382-003-0342-4

Laprise RRDE, De Elia R, Caya D, Biner S, Lucas-Picher PH, Diaconescu E, Leduc M, Alexandru A, Separovic L (2008) Challenging some tenets of regional climate modelling. Meteorol Atmos Phys 100(1):3–22

Lee DK, Suh MS (2000) Ten-year east Asian summer monsoon simulation using a regional climate model (RegCM2). J Geophys Res: Atmos 105(D24):29565–29577

Li Z, Chen Y, Li W, Den H, Fang G (2015) Potential impacts of climate change on vegetation dynamics in Central Asia. J Geophys Res: Atmos 120(24):12345–12356

Lioubimtseva E, Cole R, Adams JM, Kapustin G (2005) Impacts of climate and land-cover changes in arid lands of Central Asia. J Arid Environ 62(2):285–308

Lucas-Picher P, Argüeso D, Brisson E, Tramblay Y, Berg P, Lemonsu A, Kotlarski S, Caillaud C (2021) Convection-permitting modeling with regional climate models: latest developments and next steps. Wiley Interdisciplinary Reviews: Climate Change 12(6):e731

Mannig B, Müller M, Starke E, Merkenschlager C, Mao W, Zhi X, Podzun R, Jacob D, Paeth H (2013) Dynamical downscaling of climate change in Central Asia. Global Planet Change 110:26–39

Muñoz Sabater J (2019) ERA5-Land hourly data from 1981 to present. Copernicus Climate Change Service (C3S) Climate Data Store (CDS). (Accessed on 27-Jul-2021), https://doi.org/10.24381/cds.e2161bac

New M, Hulme M, Jones P (1999) Representing twentieth-century space–time climate variability. Part I: development of a 1961–90 mean monthly terrestrial climatology. J Climate 12:829–856. https://doi.org/10.1175/1520-0442(1999)012%3c0829:RTCSTC%3e2.0.CO;2

New M, Hulme M, Jones P (2000) Representing twentieth-century space–time climate variability. Part II: development of 1901–96 monthly grids of terrestrial surface climate. J clim 13(13):2217–2238

Ozturk T, Altinsoy H, Türkeş M, Kurnaz ML (2012) Simulation of temperature and precipitation climatology for the Central Asia CORDEX domain using RegCM 4.0. Climate Res 52:63–76. https://doi.org/10.3354/cr01082

Ozturk T, Turp MT, Türkeş M, Kurnaz ML (2016) Projected changes in temperature and precipitation climatology of Central Asia CORDEX Region 8 by using RegCM4. 3.5. Atmos Res 183:296–307. https://doi.org/10.1016/j.atmosres.2016.09.008

Paeth H, Born K, Podzun R, Jacob D (2005) Regional dynamical downscaling over West Africa: model evaluation and comparison of wet and dry years. Meteorol Z 14(3):349–367

Paeth H, Born K, Girmes R, Podzun R, Jacob D (2009) Regional climate change in tropical and northern Africa due to greenhouse forcing and land use changes. J Climate 22(1):114–132

Paeth H, Müller M, Mannig B (2015) Global versus local effects on climate change in Asia. Clim Dyn 45(7):2151–2164

Palazzi E, Von Hardenberg J, Provenzale A (2013) Precipitation in the Hindu-Kush Karakoram Himalaya: observations and future scenarios. J Geophys Res: Atmos 118(1):85–100

Perelet R (2007) Central Asia: background paper on climate change. Fighting climate change: Human solidarity in a divided world, UNDP Human Development Report, 2008

Pfeifer S (2006) Modeling cold cloud processes with the regional climate model REMO, PhD thesis, Reports on Earth System Science, Max Planck Institute for Meteorology, Hamburg, Germany

Prein AF, Gobiet A (2017) Impacts of uncertainties in European gridded precipitation observations on regional climate analysis. Int J Climatol 37(1):305–327

Prein AF, Langhans W, Fosser G, Ferrone A, Ban N, Goergen K et al (2015) A review on regional convection-permitting climate modeling: demonstrations, prospects, and challenges. Rev Geophys 53(2):323–361

Prein AF, Gobiet A, Truhetz H et al (2016) Precipitation in the EURO CORDEX 0.11◦0.11◦ and 0.44◦0.44◦ simulations: high resolution, high benefits? Clim Dyn 46:383–412. https://doi.org/10.1007/s00382-015-2589-y

Pritchard HD (2017) Asia's glaciers are a regionally important buffer against drought. Nature 545(7653):169–174

Rachmayani R, Prange M, Schulz M (2015) North African vegetation–precipitation feedback in early and mid-Holocene climate simulations with CCSM3-DGVM. Clim Past 11(2):175–185

Reick CH, Raddatz T, Brovkin V, Gayler V (2013) Representation of natural and anthropogenic land cover change in MPI-ESM. J Adv Model Earth Syst 5:459–482. https://doi.org/10.1002/jame.20022,a,b,c

Remedio AR, Teichmann C, Buntemeyer L, Sieck K, Weber T, Rechid D, Hoffmann P, Nam C, Kotova L (2019) Jacob, D (2019) Evaluation of new CORDEX simulations using an updated Köppen-Trewartha climate classification. Atmosphere 10:726. https://doi.org/10.3390/atmos10110726

Reyer CP, Otto IM, Adams S, Albrecht T, Baarsch F, Cartsburg M, Coumou D, Eden A, Ludi E, Marcus R, Mengel M (2017) Climate change impacts in Central Asia and their implications for development. Reg Environ Change 17(6):1639–1650

Roeckner E, Arpe K, Bengtsson L, Christoph M, Claussen M, Dümenil L, Esch M, Giorgetta M, Schlese U, Schulzweida U (1996) The atmospheric general circulation model Echam-4: model description and simulation of the present day climate, Report No. 218, Max-Planck-Institute for Meteorology: Hamburg, Germany

Rummukainen M (2010) State-of-the-art with regional climate models. Wiley Interdisciplinary Reviews: Climate Change 1(1):82–96

Rummukainen M, Rockel B, Barring L, Christensen JH, Reckermann M (2015) twentyfirst century challenges in regional climate modeling. Bull Am Meteorol Soc 96:ES135–ES138

Russo E, Kirchner I, Pfahl S, Schaap M, Cubasch U (2019) Sensitivity studies with the regional climate model COSMOCLM 5.0 over the CORDEX Central Asia Domain. Geosci Model Dev 12:5229–5249. https://doi.org/10.5194/gmd-12-5229-2019

Schneider U, Becker A, Finge P, Meyer-Christoffer A, Ziese M (2018) GPCC full data monthly product version 2018 at 0.25◦: monthly land-surface precipitation from rain-gauges built on GTS-based and Historical Data, Global Precipitation Climatology Centre (GPCC) at Deutscher Wetterdienst. https://doi.org/10.5676/DWD_GPCC/FD_M_V2018_025

Seddon AW, Macias-Fauria M, Long PR, Benz D, Willis KJ (2016) Sensitivity of global terrestrial ecosystems to climate variability. Nature 531:229–232. https://doi.org/10.1038/nature16986

Semmler T, Jacob D, Schlünzen KH, Podzun R (2004) Influence of sea ice treatment in a regional climate model on boundary layer values in the Fram Strait region. Mon Weather Rev 132:985–999. https://doi.org/10.1175/1520-0493(2004)132%3c0985:IOSITI%3e2.0.CO;2

Shi Y, Yu M, Erfanian A, Wang G (2018) Modeling the dynamic vegetation–climate system over China using a coupled regional model. J Clim 31(15):6027–6049

Sieck K (2013) Internal variability in the regional climate model REMO (Doctoral dissertation, Universität Hamburg Hamburg)

Small EE, Giorgi F, Sloan LC (1999) Regional climate model simulation of precipitation in central Asia: mean and interannual variability. J Geophys Res: Atmos 104(D6):6563–6582

Sofiadis G, Katragkou E, Davin EL, Rechid D, de Noblet-Ducoudre N, Breil M, Cardoso RM, Hoffmann P, Jach L, Meier R, Mooney P (2021) Afforestation impact on soil temperature in regional climate model simulations over Europe. Geoscientific Model Development Discussions, pp 1-35. https://doi.org/10.5194/gmd-2021-69

Sun Q, Miao C, Duan Q, Ashouri H, Sorooshian S, Hsu KL (2018) A review of global precipitation data sets: data sources, estimation, and inter-comparisons. Rev Geophys 56:79–107. https://doi.org/10.1002/2017RG000574

Teichmann C (2010) Climate and air pollution modelling in South America with focus on megacities, Max-Planck-Institute for Meteorology: reports on Earth System Science, Hamburg

Top S, Kotova L, De Cruz L, Aniskevich S, Bobylev L, De Troch R, Gnatiuk N, Gobin A, Hamdi R, Kriegsmann A, Remedio AR (2021) Evaluation of regional climate models ALARO-0 and REMO2015 at 0.22 resolution over the CORDEX Central Asia domain. Geosci Model Dev 14:1267–1293. https://doi.org/10.5194/gmd-14-1267-2021

Unger-Shayesteh K, Vorogushyn S, Merz B, Frede HG (2013) Water in Central Asia-perspectives under global change. Global and Planetary Change 110(Part A):1–152

Vermote E, NOAA CDR Program (2019) NOAA Climate Data Record (CDR) of AVHRR Leaf Area Index (LAI) and Fraction of Absorbed Photosynthetically Active Radiation (FAPAR), Version 5. NOAA National Centers for Environmental Information. https://doi.org/10.7289/V5TT4P69

Wang Y, Leung LR, McGregor JL, Lee DK, Wang WC, Ding Y, Kimura F (2004) Regional climate modeling: progress, challenges, and prospects. J Meteorol Soc Jpn 82:1599–1628

Wang Y, Feng J, Luo M, Wang J, Yuan Q (2020) Uncertainties in simulating Central Asia: sensitivity to physical parameterizations using WRF. Int J Climatol 40:5813–5828. https://doi.org/10.1002/joc.6567

Wilhelm C, Rechid D, Jacob D (2014) Interactive coupling of regional atmosphere with biosphere in the new generation regional climate system model REMO-iMOVE. Geosci Model Dev 7:1093–1114. https://doi.org/10.5194/gmd-7-1093-2014

Willmott CJ (1982) Some comments on the evaluation of model performance. Bull Am Meteorol Soc 63(11):1309–1313

Xu Z, Hou Z, Han Y et al (2016) A diagram for evaluating multiple aspects of model performance in simulating vector fields. Geosci Model Devel 9:4365–4380

Zhang X, Liu X, Chen J, Tang Q, Wang Y (2022) Responses and feedbacks of vegetation dynamics to precipitation anomaly over the semiarid area of North China: evidences from simulations of the WRF-Noah model. Int J Climatol. https://doi.org/10.1002/joc.7830

Zhu X, Zhang M, Wang S, Qiang F, Zeng T, Ren Z, Dong L (2015) Comparison of monthly precipitation derived from high-resolution gridded datasets in arid Xinjian, central Asia. Quatern Int 358:160–170. https://doi.org/10.1016/j.quaint.2014.12.027

Zhu X, Wei Z, Dong W, Ji Z, Wen X, Zheng Z, Yan D, Chen D (2020) Dynamical downscaling simulation and projection for mean and extreme temperature and precipitation over central Asia. Clim Dynam 54:3279–3306. https://doi.org/10.1007/s00382-020-05170-0